FEATURE ARTICLE

The C_{60} Formation Puzzle "Solved": QM/MD Simulations Reveal the Shrinking Hot Giant Road of the Dynamic Fullerene Self-Assembly Mechanism

Stephan Irle,* Guishan Zheng, Zhi Wang, and Keiji Morokuma*

Cherry L. Emerson Center for Scientific Computation and Department of Chemistry, Emory University, Atlanta, Georgia 30322

Received: February 23, 2006; In Final Form: May 9, 2006

The dynamic self-assembly mechanism of fullerene molecules is an irreversible process emerging naturally under the nonequilibrium conditions of hot carbon vapor and is a consequence of the interplay between the dynamics and chemistry of polyyne chains, π-conjugation and corresponding stabilization, and the dynamics of hot giant fullerene cages. In this feature article we briefly present an overview of experimental findings and past attempts to explain fullerene formation and show in detail how our recent quantum chemical molecular dynamics simulations of the dynamics of carbon vapor far from thermodynamic equilibrium have assisted in the discovery of the combined size-up/size-down "shrinking hot giant" road that leads to the formation of buckminsterfullerene C_{60}, C_{70}, and larger fullerenes. This formation mechanism is the first reported case of order created out of chaos where a distinct covalent bond network of an entire molecule is spontaneously self-assembled to a highly symmetric structure and fully explains the fullerene formation process consistently with all available experimental observations a priori. Experimental evidence suggests that it applies universally to all fullerene formation processes irrespective of the carbon source.

1. Introduction

The boom of fullerenes and carbon nanotubes (CNTs, originally called "buckytubes") in the early 1990s lent the sprouting new scientific discipline of nanotechnology fresh food and rationale.[1,2] It is therefore all the more surprising that we know very little today about the atomic level formation mechanisms of these important self-assembled carbon nanostructures. This work presents a review of the current knowledge on fullerene formation and related reactions and introduces the "shrinking hot giant" road of fullerene formation, which describes a dynamic fullerene self-assembly mechanism we discovered in quantum chemical molecular dynamics (QM/MD) simulations of hot carbon vapor in a nonequilibrium environment. The shrinking hot giant road consists of two parts: a "size-up" part, where giant fullerenes are self-assembled by the interplay of dynamics and chemistry of hot polyyne chains in carbon vapor leading to exothermic, more or less curved π-stabilized sp^2-networks, and a "size-down" part, where these giant, vibrationally excited cages shrink down to the size of C_{70} and C_{60}. As we will show, this combined mechanism matches experimental observations and explains the formation of the beautiful, highly symmetric C_{60} structure in a chaotic, hot reaction system. Of course we are aware that "victory" has been proclaimed several times in the front of C_{60} formation research, but our work marks the first time that direct atomistic evidence is reported in a priori molecular dynamics simulations based on a true quantum chemical potential.

* Corresponding authors. E-mail: sirle@emory.edu; morokuma@emory.edu.

This paper is organized as follows. First, in the remaining paragraphs of section 1 we briefly review the history of buckminsterfullerene C_{60} (BF), giant fullerenes, and experiments involving fullerene shrinking, early theoretical calculations, and miscellaneous experimental observations. Section 2 describes previously proposed hypothetical fullerene formation models, and section 3 reports previous computational investigations of fullerene formation. Section 4 touches briefly on the relationship between open environments and emergent phenomena in nonequilibrium thermodynamic systems, and section 5 is devoted to the shrinking hot giant road of fullerene formation itself. We close in section 6 with conclusions and an outlook on future studies addressing remaining minor open questions.

A. The History of Buckminsterfullerene, Giant Fullerenes, and Fullerene Cage Shrinking. *The Experimental History of Buckminsterfullerene.* The discovery of the buckminsterfullenene C_{60} molecule in a mass spectrum and the now world-famous proposed icosahedral soccer ball structure was first reported by Nobel Prize winners Harry Kroto, Richard Smalley, Robert Curl, et al. in a work from 1985,[3] which features the photograph of a soccer ball, signifying the importance of this universal and near perfect spherical structure. Their simple, yet brilliant structural proposal is the only ingredient setting their work apart from the earlier report of an Exxon group which also contains a prominent C_{60} peak in their mass spectrum.[4] At the time, the discovery of the C_{60} soccer ball cage-like molecular structure came somewhat as a surprise because originally the research team around Smalley and Kroto had set out to study long carbon chains observed in interstellar clouds,[3] using a powerful pulsed Nd:YAG laser, which was state-of-the-art technology. To their

10.1021/jp061173z CCC: $33.50 © 2006 American Chemical Society
Published on Web 06/17/2006

Stephan Irle obtained his diploma in chemistry at the University of Siegen in Germany and a Ph.D. from the University of Vienna in Austria. Starting from 1997, he has worked with Prof. Keiji Morokuma at Emory University on many problems in theoretical and computational chemistry, from small-molecule gas-phase reactions to large-scale quantum chemical molecular structure investigations. Recently he has coordinated the Computational Nanomaterials Research efforts of the Morokuma group and increasingly used quantum chemical molecular dynamics simulations in the study of nanomaterial self-assembly processes far from thermodynamic equilibrium.

Guishan Zheng received his Master's degree in polymer science and physics in 2001, working under the direction of Prof. Xue Gi in Nanjing University, China. He is going to receive his Ph.D. degree in 2006 under the advice of Prof. Keiji Morokuma at Emory University. His research interest in Ph.D. study is mainly focused on nanoscale chemistry and the development of density functional based tight binding method. In August 2006, he will join Prof. Todd Martinez' group at UIUC as a postdoc.

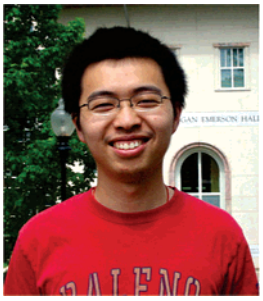

Zhi Wang obtained his Bachelor's degree from University of Science and Technology of China in 2004. Currently he is a graduate student in the Department of Chemistry at Emory University. His research interest lies on the DFTB-based QM/MD simulations of formation mechanisms of fullerenes and carbon nanotubes.

Keiji Morokuma is a William H. Emerson Professor of Chemistry and Director of Emerson Center at Emory University. Having obtained his academic degrees from Kyoto University, he was a professor at University of Rochester and Institute for Molecular Science at Okazaki, Japan, before taking up his present appointment at Emory. Prof. Morokuma has authored over 570 scientific publications and has received numerous scientific awards, including Japan Chemical Society Award, Schrödinger Medal from World Association of Theoretical Organic Chemists, and Fukui Medal of Asian Pacific Association of Theoretical & Computational Chemists. He is the President of International Academy of Quantum Molecular Science.

amazement, instead of polyyne chains they found carbon clusters of large sizes, with C_{60} and C_{70} in an approximate 5:1 ratio[5,6] obviously representing "magic numbers" in the mass spectrum of the ionized products. The postulated soccer ball structure became finally established with the successful extraction of macroscopic quantities of C_{60} and its IR and UV spectroscopic characterization by Krätschmer and Huffman in 1990,[7,8] and its NMR spectrum by Kroto,[9] and Smalley, Kroto, and Curl received the 1996 Nobel Prize in Chemistry.

Giant Fullerenes. Due to its abundance and elegant, simple, and highly symmetric design, C_{60} has become the paradigm of fullerenes, although larger even-numbered fullerenes such as C_{70}[6,7] up to C_{250}[10] were isolated and characterized almost at the same time as their more famous soccer ball cousin. In fact, even numbered fullerenes up to C_{600} and even larger have been reported early on,[11,12] and it is now well established that so-called giant fullerenes (GFs)[13,14] exist in great numbers and variety. Smalley stated in 1992 that "a bit more work to probe the nature of the larger carbon clusters would have been fruitful during those years".[15] As we now know, GF aggregates occur frequently as multi-shell graphitic onions or spiroids[14,16−20] in carbon soot, and recently even micrometer-sized graphite balls have been reported in both pure carbon[21] and hydrocarbon[22] environments.

Experiments Investigating Fullerene Cage Shrinking. Perhaps following their very human nature, the "Rice team" around Smalley set out to destroy the obviously very sturdy C_{60} cage[23] and its metal-containing complexes[24] almost immediately after their discovery, using laser-induced photodissociation experiments.[25] In these experiments it was found that carbon clusters containing more than 34 atoms lose preferably C_2 units and C atoms for even and odd numbers of carbon atoms, respectively, requiring high (12.8 eV, 295 kcal/mol or higher) excitation energies. They proposed a Woodward−Hoffmann forbidden C_2 elimination process from two abutting pentagons (denoted as a 5/5 situation), leading to the formation of a 5/6/5-membered fused ring combination. Stanton later performed semiempirical MNDO calculations[26] and found that a necessary prerequisite for the C_2 eliminations to be energetically feasible is a preceding Stone−Wales (SW) type transformation, involving the rotation of a C_2 unit to create a pair of 5/7-membered fused rings.[27] This proposed mechanism of C_2 elimination from fullerene defects became later known and famous as "shrink-wrap" mechanism.[15,28,29]

Several research teams investigated what happened when fullerene cations were exposed to bombardment with rare gas atoms,[30−33] and also observed C_2 and C_4 elimination reactions.[31] In particular, Ehlich et al. reported a relatively low-energy C_2 elimination maximum of around 20 eV (466 kcal/mol) kinetic energy for He collisions with C_{60}, based on molecular dynamics (MD) simulations.[32] The C_2 unit itself has an unusually high heat of formation with 200 kcal/mol,[34] which is certainly an important driving force for its relatively easy elimination. The

most accurate experimental binding energy of C_2 in C_{60} was reported by Lifshitz et al. and is in excess of 10 eV (231 kcal/mol).[35]

B. Early Theoretical Fullerene Investigations. Theoretical exploration of fullerenes began 15 years before the experimental discovery of C_{60}, when Eiji Osawa postulated its existence and stability,[36−38] inspired by watching his son play with a soccer ball. He introduced a hypothetical concept termed "superaromaticity" which describes lowering of energy by delocalization of π-molecular orbitals over some three-dimensional surface of high symmetry.[36,38] Bochvar and Gal'pern published a theoretical study on C_{60} in 1972[39] and later in 1984 with soccer fan Ivan Stankevich.[40] It did not take theoreticians long to realize that the soccer ball skeleton of the C_{60} molecule naturally obeys the important isolated pentagon rule (IPR)[41−43] as smallest icosahedral fullerene with 12 pentagons, which lends remarkable thermodynamic stability to its structure.

Ironically, however, it is now consensus that C_{60} does not exhibit superaromaticity, as its resonance energy per π electron is only 60% of that of benzene, according to Aihara's topological theory of aromaticity.[44] To make matters worse, it has been shown that a free electron gas bound on the surface of a sphere with $2(N+1)^2$ electrons is in a closed-shell electronic configuration,[45,46] and Hirsch et al. found[47] that neutral and charged fullerenes with $2(N+1)^2$ π electrons exhibit large negative nucleus independent chemical shifts (NICS), considered to be an important criterion for aromaticity according to Schleyer et al.[48] Alas, C_{60} does not belong in the $2(N+1)^2$ class of molecules, and neither does C_{70}! Moreover, simple Hückel theory,[49] MNDO,[50,51] and DFT[52,53] calculations predict the closed-shell D_{5h} isomer of C_{70} to be more stable than I_h C_{60}, with both their delocalization energies being close to that of graphite.[49]

C. Why Is C_{60} So Abundant? A Closer Look at Hot Carbon Vapor. So, why is the C_{60} cluster so abundant in the condensation products of carbon vapor? To answer this question, we have to go back and look at the environmental conditions of fullerene formation. Besides the well-known laser vaporization,[3,54] carbon arc,[8] and hydrocarbon combustion[55,56] fullerene syntheses, C_{60} and higher fullerenes have been found and characterized as byproducts of SWNT formation,[57,58] at locations of asteroid impacts on Earth,[59−61] lightning strikes,[62,63] ancient brush fires,[64] and of course in ordinary candle flames.[65] All these findings seem to imply that carbon-rich material and very high temperatures (>1000°C) are about the only requirements for fullerenes to form spontaneously.

The creation of C_2, C_3, and other smaller carbon linear clusters and rings at early stages in carbon vapors and plasmas is a subject that is a recurrent topic in the literature,[66−82] inspiring Kroto to the "party line" mechanism of fullerene formation.[83] Inevitably, carbon vapor condensation follows a direction from high-energetic sp-hybridized carbon species to lower-energetic sp^2-hybridized finite size graphene clusters. The aggregation of small chains and rings[70,71,83−86] to condensed ring systems with trivalent carbon atoms[71,72] and further on the formation of fully sp^2-hybridized graphene sheets is highly exothermic[87] and occurs very rapidly. The role of the carrier gas during chain growth and condensation is to remove excess heat[88] and expand the carbon vapor plume, but it may also play a role in "knock-off" events of C_2 and C_4 units,[31,33] where bulky large carbon structures are seemingly "sandblasted" to assume more streamlined shapes. Under these conditions, singlet C_{60} and higher fullerenes with smooth, closed surfaces and low ring strain are a thermodynamically attractive structural choice for cooling finite-sized sp^2-hybridized carbon clusters.[89]

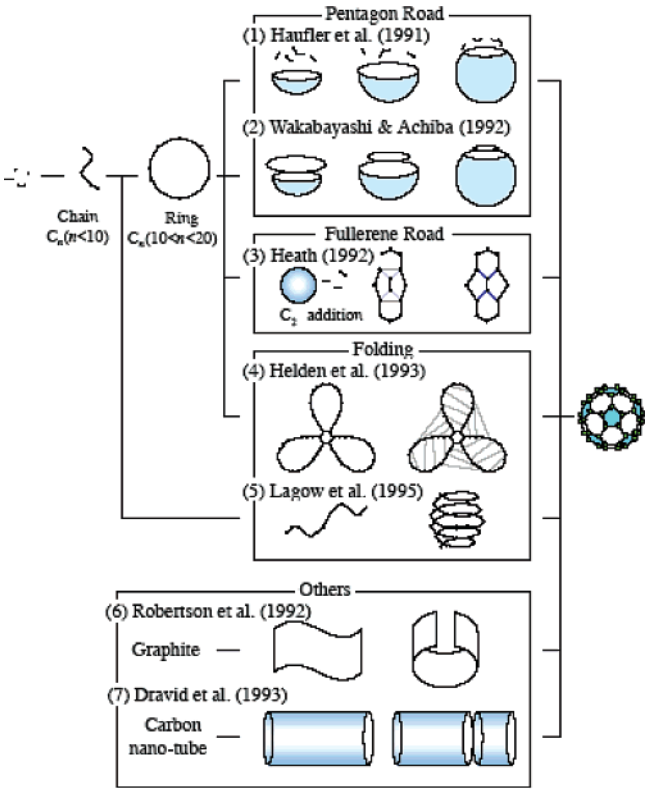

Figure 1. Schematic diagram of hypothetical fullerene formation models according to Maruyama. Used with permission from ref 102.

2. Hypothetical Models of Fullerene Formation: The Puzzle Remained Unsolved

Hypothetical models of fullerene and carbon nanotube formation mechanism are abundant in the literature and often are only small variations of previously proposed ones. The most basic and prominent models for fullerene formation mechanisms are, in chronological order, the "nautilus model"[12,90] and its close relative, the "accreting snowball model",[20] the "pentagon road",[15,28,91] the "fullerene road",[92] the "party line" mechanism of fullerene formation,[83] the "ring-stacking" mechanism,[93,94] the very popular "ring fusion spiral zipper" mechanism,[71,72,95−97] and recently the Kvataron model.[98] One hypothesis even suggested that fullerenes are created by fragmentation of CNTs.[99] Reviews of refs 100 and 101 give an overview of the earlier proposed formation mechanisms. As shown in Figure 1, Maruyama et al.[102] have classified these models as members of four fundamentally different concepts: (a) the "pentagon road", where basket-like structures grow into spheres by intermolecular addition of smaller carbon units under incorporation of pentagons (nautilus model, pentagon road, ring stacking); (b) the "fullerene road", which is based on the growth of smaller fullerenes by C_2 insertion but does not solve the problem where they should come from; (c) folding models (ring fusion spiral zipper, also sometimes called "ring collapse"), where fullerene cages are "knitted" intramolecularly following ring condensation reactions involving $sp \rightarrow sp^2$ transformations, first proposed for chemical fullerene synthesis by Rubin et al.;[103,104] and (d) others. All of these models share the underlying assumption of a "blueprint" or "road map" associated with intermediate structures that are in thermodynamic equilibrium. Not a single model has considered that hot carbon vapor is a system far from

thermodynamic equilibrium, and that such systems may give rise to autocatalysis and self-organization processes associated with irreversible processes, as was shown in the pioneering work of Prigogine et al.[105]

Concerning fullerene and soot formation in hydrocarbon combustion, the above-mentioned models do not strictly apply, as the presence of hydrogen has to be considered in the fullerene self-assembly process. Homann has given a comprehensive review on the topic,[106] based mainly on his extensive mass spectroscopic analysis of acetylene and benzene flames,[55,65,107−109] which are composed of (a) aromatic radicals such as phenyl, benzyl, indenyl, naphthyl, and phenoxy, (b) aliphatic radicals including ethynyl, C_2, C_3H, and carbenes CH_2, C_3H_2, and C_5H_2,[108] and (c) larger polyaromatic hydrocarbons (PAHs) with up to 600 carbon atoms or even more.[106,107] Since the C_2 concentration in flames is very small,[108,110] Homann et al. have therefore speculated that fullerene cages are formed through aggregation of hydrogen-containing PAH radicals and their subsequent oxidation by oxygen, reducing gradually the H/C ratio and introducing pentagons by CO elimination from hexagons.[106] Again, this "road map" follows strictly thermodynamic equilibrium pathways, and does not explain how a regular, symmetric body like C_{60} is self-assembled with great consistency in the chaotic mixture of hot PAHs.

3. Previous Computational Investigations of Fullerene Formation

In the following two subsections, we briefly review past exclusively computational investigations of the fullerene formation mechanism based on the quantum chemical study of reaction pathways for simple model systems as well as on reactive molecular dynamics simulations that use classical as well as quantum chemical potentials.

A. Reaction Pathway Approaches. In this subsection we review various reaction pathway investigations on model systems that have been attempted in order to study C_{60} formation from smaller to larger clusters as well as from larger to smaller fullerene cages, all of which are designed to consider experimental observations as close in spirit as possible. The daunting words of Smalley always accompanied such studies of reaction pathway mechanisms: "Of course there must be hundreds of mechanisms whereby a fullerene like C_{60} can form",[15] and sadly, even this must be considered a severe understatement.

Semiempirical Studies of Fullerene Formation Pathways. Mishra et al. attempted to locate transition state structures connecting intermediate structures and describing entire pathways for the formation of C_{28} fullerene through their "ring-collapse" mechanism at the semiempirical AM1[111] level of theory, starting from small monocyclic carbon rings such as C_9 and C_{13}.[112] Remarkably, in all their reaction pathways, a huge energetic barrier in excess of 100 kcal/mol was encountered when C_{28} had to become bent in order to finally close and gain the π-conjugation resonance stabilization. This finding is notorious for any attempt to close small fullerene cages C_n from compounds containing n carbon atoms, as has also been demonstrated for C_{24},[113] and the first steps toward C_{26} and C_{36}.[114] It is more than questionable that nature would choose to consistently follow reaction pathways that are associated with such high energy barriers, as this would imply that the growing carbon cluster somehow "knows" beforehand about the favorable energy stabilization achieved in the end by cage closure and somehow deliberately works on the closing process.

Ab Initio and First Principles Studies of Fullerene Formation Pathways. Scuseria et al. investigated a cycloaddition model of fullerene formation, looking at a variety of 2+2, 2+4, and 4+6 cycloadducts of monocyclic rings,[115] following the ring fusion spiral zipper model,[71,72,95,97] using DFT. Later, they investigated intermediate structures that would occur as intermediates in the pentagon road to BF using a similar methodology.[116] Jones studied the structures of carbon clusters up to C_{32}, including chains, rings, cages, and graphitic isomers.[117] In the same year, Portmann et al. published a comprehensive DFT study on isomers of C_{28}.[118] As to carbon clusters C_n with increasing size n, DFT studies have consistently pointed out that larger fullerenes are more stable than smaller ones on a per atom basis and that corresponding graphene sheets represent the global C_n minimum.[52,53] This theoretical result is in agreement with enthalpies of formation for graphite[119] and C_{60} (ref 120) and can be interpreted such that the pentagons necessary for fullerene curvature represent local graphene defects, each increasing the energy by more than 45 kcal/mol.[53]

Concerning C_{60} formation under PAH combustion conditions, Takano et al. have suggested a reaction pathway starting from six naphthalene units and their fusion products, based on AM1 and Hartree−Fock calculations that suggest an overall reaction barrier of 60 to 70 kcal/mol for this radical pathway.[121] However, requirement for this assembly is precise connection of the correct bonds among the six naphthalene fragments, which seems very unlikely given the huge number of possibilities for such a fusion process.

Despite the success of DFT calculations in predicting the heat of formation for C_{60},[52,53] it is puzzling how widely carbon cluster isomer energetics can be scattered according to different quantum chemical methods, as large differences up to 100 kcal/mol, for instance for the C_{20} cage, bowl, and ring isomers, are obtained at the DFT, MP2, coupled cluster,[122] quantum Monte Carlo,[123] and multireference MRMP2[124] levels of theory (see ref 123 for an excellent comprehensive overview). Much more work has been reported which simply cannot be reviewed here.

Calculations of Shrink-Wrap C_2 Elimination from Fullerene Cages. Apart from the already mentioned seminal MNDO calculations of Stanton,[26] Scuseria et al. have made a significant contribution to investigate the shrink-wrap mechanism by computing the binding energy of C_2 in C_{60} at the DFT and MP2 levels of theory.[125] Their paper entitled in part "theory disagrees with most experiments" gives a nice overview over previous theoretical and experimental results, pointing out that HF and DFT/MP2 disagree on the lowest energetic isomer of C_{58}, and predicts the C_2 elimination energy from C_{60} to be 11.2 eV (258 kcal/mol) at the most accurate MP2 level of theory. This value has later been confirmed by Lifshitz et al. who estimated the binding energy experimentally to be greater than 10 eV (231 kcal/mol).[35] Kappes et al. have computed the binding energy for the reaction $C_{70} \rightarrow C_{60} + 5C_2$ from thermodynamic data[126] to be 8.1 eV (187 kcal/mol), indicating that C_2 loss from larger fullerenes might be substantially easier than from C_{60} by at least 50 kcal/mol.

It is interesting to note that recent B3LYP calculations suggest the insertion process to be quasi-elastic if the reaction heat is not absorbed by third body collisions and that fullerene growth by C_2 insertion is in fact an unlikely process.[127,128] C_2 elimination therefore can be considered irreversible.

B. Reactive Monte Carlo and Molecular Dynamics Simulations. Monte Carlo (MC) and molecular dynamics (MD) simulations are ideally suited to describe the dynamics of complex systems and are therefore popularly employed in the context of biochemistry or materials chemistry. Unfortunately, if one wants to study chemical transformations that include bond

formation or breaking, reactive MD simulations are required, and there are currently only two flavors of force fields available in hydrocarbon chemistry that are capable to describe chemical reactions: the fairly recent ReaxFF force field of Goddard et al.[129] and the reactive empirical bond order (REBO) potential developed by Brenner.[130−133] Certain terms in the functional form of the REBO potential have later been improved,[134,135] but these relatively minor modifications have never been employed in investigations of the fullerene formation mechanism. QM/MD simulations are therefore certainly preferable but are several orders of magnitude computationally more expensive.

REBO Monte Carlo and MD Simulations. Realizing the vast number of carbon cluster isomers one faces in the study of fullerene formation, MC and MD simulations became popular investigative methods starting from 1990. Ballone and Milkani used the REBO potential to study the annealing of carbon clusters C_n with $50 \leq n \leq 72$ from 4000 K in MC simulations.[136] However, artificially, the carbon atoms were all placed on the surface of a sphere, and stable C_{60} and C_{70} isomers were found. The first MD simulation study of fullerene formation is perhaps the one by Brenner et al. in 1992.[137] In this work, the importance of pentagon formation and high temperature for the curling and closure of a graphitic ribbon was pointed out, but the origin of such a hypothetical ribbon was not addressed. Chelikovsky found in the same year that the initial phase of C_{60} cage formation is dominated by nucleation of polyyne chains, when 60 carbon atoms are enclosed in a 12 Å cubic periodic boundary box and gradually annealed from 7000 to 2000 K;[138] however, in his studies a REBO-like potential had been altered to allow favorable "buckling". Schweigert et al. performed REBO MC and MD simulations along the line of the ring fusion spiral zipper mechanism by heating hexagon-bound tricyclic structures but could not find anything special about cages C_{60} and C_{70} formed in this way when compared to other size carbon clusters.[139]

In the late 1990s, Maruyama et al. performed REBO-based MD simulations to study the formation of BF, using cubic periodic boundary boxes of 30 Å side length filled with 500 carbon atoms.[102,140−143] Their target temperature was 1500 K, and indeed carbon cluster growth up to C_{70} and larger was observed on the order of nanoseconds simulation time. The most serious problem in these simulations is the fact that carbon clusters seem to grow continuously over time, and especially C_{60} clusters are bound to grow even larger provided the simulation is continued. Nevertheless, the Maruyama group's REBO simulations are important pioneering work in the theoretical investigation of the fullerene formation mechanism, honestly trying to simulate the hot carbon vapor environment without adding any assumptions that would artificially favor the formation of carbon cages. In that sense, the later MSXX FF dynamics simulations by Goddard et al. on isolated carbon clusters from C_{20} to C_{60} represented a step back in the attempt to simulate the fullerene self-assembly process.[144]

Concerning simulations of PAH combustion processes, Violi et al. have recently performed multiscale coarse-grained MD simulations[145] of nanoparticle aggregates during soot formation, investigated H abstraction from PAHs by hydrogen atoms at the DFT level of theory,[146] and used a kinetic model with 492 reactions involving PAH radicals to study the molecular growth process in aromatic and aliphatic flames. However, Violi et al. also fail to explain why C_{60} is so abundant, as there is no evidence in their simulations as well that particle growth should magically stop at $n = 60$.

Tight-Binding MD Simulations. REBO and ReaxFF molecular force fields do not take into account π-conjugational effects. However, π-conjugational stabilization is one of the most important factors in the chemistry of sp^2 hybridized carbons, as is well-known in the reactivity of aromatic hydrocarbons.[147,148] Therefore it is essential to perform on-the-fly electronic structure trajectory calculations that have become recently popular for the treatment of moderately sized systems, such as tight-binding, ab initio DFT, or Car−Parinello MD simulations.

Wang et al. have first used TBMD simulations in 1992 to study the formation mechanism of fullerenes, using 60 carbon atoms at up to 6000 K temperature, and included a spherical reflection potential.[149] They found only stable closed cage formation if the radius of this sphere was 3.382 Å, at temperatures up to 5000 K. More recently, Laszlo reported a TBMD study where 60 carbon atoms and 1372 helium atoms were annealed from 12000 K down to 500 K in a cubic periodic boundary box that was gradually shrunk to 25 Å side length.[150] They found that an initial 6-24-24-6 slab sandwich arrangement of the 60 carbon atoms mentioned first by Kroto[151] immediately was transformed into polyyne chains, and that fused pentagons and hexagons appeared later as a result of interchain interactions, leading to caged structures after about 20 ps. This is consistent with findings by Lee et al., who performed tight-binding based action-derived MD (ADMD) simulations on C_{60} isomers, also reporting that the "existence of chains in the models of tangled polycyclics and open cages is beneficial for the formation of C_{60} molecule."[152] After our work on the self-assembly mechanism of giant fullerenes was published,[153−155] similar TBMD simulations of carbon droplets with up to 240 atoms at 3500 K were reported in which similarly giant fullerenes with both even and odd number of carbon atoms self-assembled from polyyne chains.[156] Besides the tight-binding based studies, we have not found any ab initio or DFT MD study of the fullerene formation mechanism in the literature.

4. Nonequilibrium Conditions, Irreversible Processes, and Emergent Structures

For a phenomenon to be termed emergent it should generally be unpredictable from a lower level description. Usually the phenomenon does not exist at all or only in trace amounts at the very lowest level: it is irreducible. Nobel laureate Ilya Prigogine and his research groups have impressively shown in a large body of works that physical systems under nonequilibrium conditions behave very differently from the time-reversible behavior exhibited under equilibrium conditions, and in particular that autocatalysis and self-organization are emergent phenomena frequently encountered in systems open to matter and/or energy flow.[105,157,158] These self-organization processes then create "dissipative" ordered structures, corresponding to dynamic states of matter characterized by the interaction of a given system with its surroundings, and occur both in time and space. Famous examples of dissipative structures are observable in the Belousov−Zhabotinsky reaction[159] and in Rayleigh−Benard convection cells.[160] Moreover, according to Boltzmann's famous equation $S = k \ln W$, probability and irreversibility are closely related, and irreversibility enters a system only when it behaves in a sufficiently random way. Irreversible processes determine the direction of time and are a necessary requirement for the creation of complex structures and order.[105] However, this phenomenon has so far never been discussed in terms of molecular self-assembly where all covalent bonds of an entire molecule are formed, partly because chemistry normally is not

studied at extreme conditions that allow the molecules to occupy a vast number of probable states with different numbers of valences in extended σ-bond networks. Hot carbon vapor seems to be exactly such a system, and it is indeed very fertile for the self-assembly of giant fullerene cages, as nature and our QM/MD simulations show. How this is achieved along the "shrinking hot giant" road will be shown in atomic level detail in the following section.

5. The "Shrinking Hot Giant" Road of Fullerene Formation

This section describes our QM/MD simulations of the dynamic fullerene self-assembly mechanism from hot carbon vapor, represented by randomly oriented ensembles of C_2 molecules at 2000 and 3000 K temperature.[153−155] First, we will briefly review our benchmark studies on the accuracy of the density functional tight binding (DFTB) method compared to ab initio DFT results, and describe the methodology of our QM/MD simulations. Then, we will elaborate on the "size-up" and "size-down" parts of the two-step shrinking hot giant road of fullerene formation, pointing out connections with experimental observations wherever applicable.

A. Computational Methodology. *Accuracy of the DFTB Method.* The DFTB method is the central method employed to compute on-the-fly potential energy surfaces (PESs) and energy gradients for direct trajectory calculations in the presented studies. All DFTB calculations were carried out with the program packages developed by Frauenheim, Seifert, and Elstner.[161−163] DFTB is an approximate density functional theory method based on the tight binding approach and utilizes an optimized minimal LCAO Slater-type all-valence basis set in combination with a two-center approximation for Hamiltonian matrix elements. Within the DFTB formalism, there are three options available. One is the self-consistent charge (SCC) formalism, in which the atomic charge−atomic charge interaction is included in the energy and the atomic charges are determined self-consistently.[163] The second is the nonself-consistent charge (NCC) option, in which the atomic charge−atomic charge interaction is neglected.[161] The third is the most time consuming option, where both atomic charges as well as spin densities are self-consistently converged (SCC-sDFTB).[164]

The original NCC-DFTB method, approximately three to seven times faster than the SCC option, is not a bad approximation for all-carbon systems such as pure SWNTs and fullerenes. Our benchmark comparison with B3LYP/6-31G(d) energetics of cage-, ring-, and polyaromatic ring-isomers of C_{28} shows this very clearly (see Table 1), and in particular we note that the parametrization of the DFTB repulsive potential allows to match energetics of B3LYP with polarized basis sets much better (R^2 = 0.76) than even B3LYP/6-31G without *d*-functions (R^2 = 0.54).[154,165] In benchmark studies on geometries and isomer energetics of fullerene cages C_{20} to C_{84}, we found similarly that the NCC option performs very reasonable in the case of neutral all-carbon systems.[166] Therefore, and because we are not including ionic species in this study, NCC-DFTB was used throughout our QM/MD simulations, and for simplicity we denote this level of theory as DFTB in the remainder of the text. The accuracy of DFTB makes our QM/MD simulations inherently more accurate than conventional TBMD simulations.

Computational Methodology of DFTB-Based QM/MD Simulations. Direct DFTB QM/MD simulations were performed by calculating analytical energy gradients on the fly, using them in a velocity Verlet integrator for time propagation. In case of hydrogen-free systems, we found that a time interval Δt of 1.209 fs (= 50 atomic units) allows energy conservation within 1 to 2 kcal/mol in Newtonian dynamics in a 9900-step microcanonical ensemble simulation for about 12 ps. This error is by far negligible considering typical simulation temperatures of 1000 K and higher. Temperature is kept constant throughout the system by scaling of atomic velocities, an overall probability 20% scaling for the entire length of the simulations. Initial velocities are assigned randomly at the beginning of each simulation; however, when fragments are added during continued trajectories, only the velocities of these fragments are randomly chosen and scaled to the target temperature. While periodic boundary conditions (PBC) are used during size-up trajectories, during size-down trajectories we have dropped the PBC to allow carbon fragments to detach freely from the cage.

TABLE 1: Relative Energies of C_{28} Isomers in [eV] and Corresponding Linear Regression Coefficient R^2 for Correlation between B3LYP/6-31G(d), and DFTB, B3LYP/6-31G, AM1, and PM3 Methods[a]

	B3LYP/6-31G(d)	DFTB	B3LYP/6-31G	AM1	PM3
buckyD2	0.00	0.00	0.00	0.00	0.00
ring	3.32	8.10	0.78	−7.69	−2.15
c24−6	3.17	3.56	1.99	0.43	1.77
2+2r14	5.08	9.66	2.90	−3.34	0.91
2+2r16	6.01	10.25	3.87	−3.37	0.90
c20−6o	5.41	5.52	4.34	3.42	4.23
c20−6 m	5.57	5.62	4.48	3.43	4.24
2 + 4	7.97	10.28	6.00	0.10	3.60
central7	5.86	6.07	4.84		
8 + 8	7.43	9.43	5.31	−3.24	0.79
4 + 4	9.91	14.27	8.52	1.52	4.97
R^2		0.7571	0.5390	0.2079	0.2964

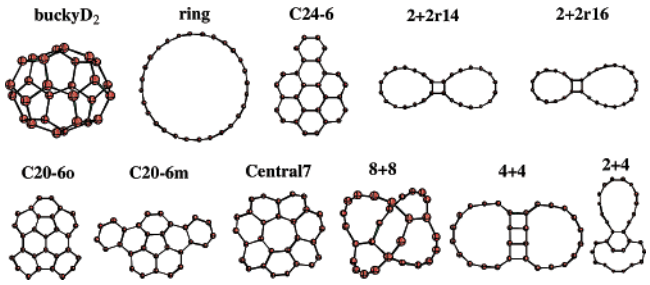

[a] All energetics are obtained using individually optimized molecular structures at respective levels. From refs 154,165. Structures of C_{28} used in the benchmark calculations presented in Table 1. From refs 154,165.

B. Self-Assembly Formation of Giant Fullerenes in Carbon Vapor: Size-Up. This step was traditionally thought to be the only process required to generate C_{60}, C_{70}, and other abundant fullerene cages directly from hot carbon-rich material and is the only subject of proposed hypothetical fullerene formation mechanisms (see section 2). Perhaps closest in explaining this process came the TBMD studies of Laszlo[150] and Lee et al.,[152] but they started out with exactly 60 carbon atoms, which is why the important detail was missed that in fact giant fullerenes (GFs) are much more easily formed than C_{60} directly. However, in many of the previously reviewed fullerene formation simulations, polyyne chains and macrocycles have been reported as abundant species, although not always explicitly mentioned,[138−143,149,150,152] supporting in part the "party line"[83] and "ring fusion spiral zipper"[71,72,95−97] hypothetical mechanisms of fullerene formation.

Polyyne Chains are Highly Abundant Species in the Chemistry of Hot Carbon. In the investigation of high-temperature dynamics of open-ended carbon nanotubes, we observed the spontaneous creation of long-lived "wobbling C_2-units" at the open ends

as a predominant feature in our QM/MD simulations,[165,167] which is in noticeable agreement with the observations of Car et al. in their computationally much more expensive CPMD studies on similar systems.[168] As mentioned in the Introduction, Smalley and Kroto et al. already pointed out very early after the discovery of BF that polyyne chains are easily created when graphite is exposed to high temperatures,[66,67] their study in fact being the original motivation for the BF C_{60} work.[3] The theoretical QM/MD and CPMD studies directly confirm that linear, sp-hybridized carbon polyyne chains are favorable species under high temperature conditions and emerge spontaneously from sp^2-hybridized graphitic systems. It is reported that Smalley mentioned during a conference that high-temperature carbon nanotube defects would resemble the threads coming out of a worn old sweater. The results of our QM/MD simulations and his alleged anticipation of such structural defects are in perfect agreement. Recently, experimental evidence for the existence of polyyne chains inside cold multiwalled carbon nanotubes (MWNTs)[169] and high-temperature coalesced double-walled carbon nanotubes (DWNTs)[170] was observed in Raman spectra, but the nature of these high-frequency Raman peaks in these low-temperature species is still debated. It is, however, clear from the combined overwhelming evidence discussed in the Introduction and from the results of QM/MD simulations mentioned above that at high temperatures polyyne chains emerge spontaneously as entropically favorable species and can take on complex tasks related to autocatalysis and self-organization.

Three-Stage Dynamic Self-Assembly Mechanism of Giant Fullerenes. Until today, macrocyclic rings of polyyne chains are widely accepted as centrally important species for fullerene formation, and as we shall see, this assumption is not far from the truth according to the results of our high-temperature nonequilibrium dynamics QM/MD simulations of the giant fullerene self-assembly mechanism from C_2 molecules.[153−155] Trajectories of these publications can be viewed or downloaded online at http://euch4m.chem.emory.edu/nano. To provide unbiased initial conditions without artificial constraints, we have started with ensembles of randomly oriented C_2 molecules placed in relatively small cubic boxes. During the dynamics, a larger PBC box size was selected and the target temperature was set to 2000 K. In the first of these studies,[153] we used 60 initial C_2 molecules in an initial 20 Å cubic box, and propagated the system in a 30 Å cubic PBC box, while in a second published study,[155] 40 initial C_2 molecules in an initial 10 Å cubic box were propagated in a 20 Å cubic PBC box to increase the carbon density by a factor of about 2. In both studies, after propagating for 6 ps, we added 10 more C_2 molecules randomly to the system, and resumed propagation (see Figure 2). The addition of more C_2 molecules was performed to (a) simulate material and energy flux in the open environment under laboratory conditions and (b) to save computer time especially at the beginning of the simulations. We repeated the C_2 addition step for a total of 5 and 3 times in low- and high-density cases, increasing the number of carbon atoms to 240 in case of **S/U** trajectories (the low-density study) and 110 in case of **W** trajectories (the high-density study) at the end of the simulations, heating to 3000 K during the final steps. Snapshots of representative "successful" trajectories are shown in Figure 3. In the case of low-density simulations, the ratio of successful/total trajectories was 5/25 = 20% with an average cage size of 162, whereas in the case of high-density simulations, the success rate was reduced to 5/100 = 5% with an average cage size of 88. We refer to the original works in refs 153 and 155 for more detailed descriptions of these simulations. Additional trajectories

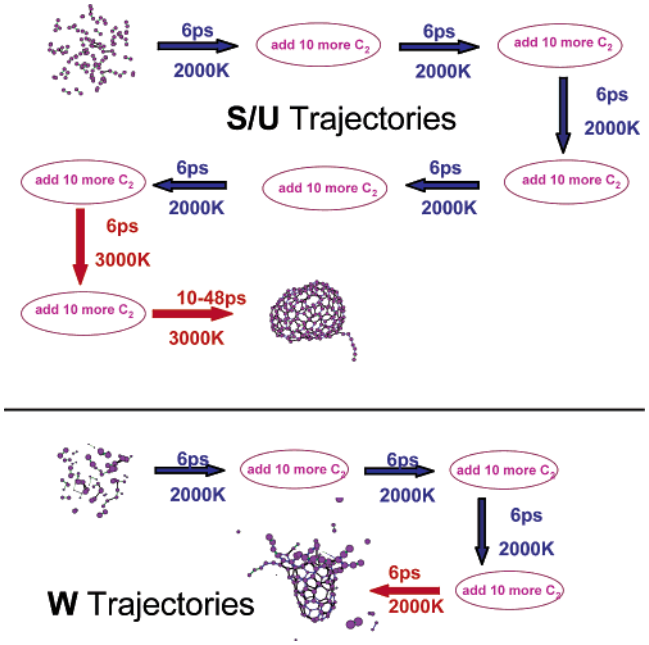

Figure 2. Schematic representation of **S/U** and **W** trajectories published in refs 153 and 155, respectively.

following similar simulation sequences carried recently out in our lab have roughly confirmed these numbers, and slower C_2 addition with time intervals of 12 ps instead of 6 ps have led to even increased fullerene yields of about 30% (named **Szn**-trajectories),[171] presumably reflecting the importance of annealing and slab self-healing.

Originally, the concept of "self-assembly" in fullerene formation emerged somewhat surprisingly but naturally as a consequence of the nonequilibrium conditions,[153−155] and we realized that fullerene cages indeed might represent "frozen" dissipative dynamic carbon structures commonly found in nonlinear dynamic systems,[105,157] trapped by fast cooling thanks to their kinetic stability. Figure 4 depicts schematically the self-assembly "size-up" mechanism of GFs from ensembles of randomly oriented C_2 molecules in our QM/MD simulations. We found that GF growth occurs in three stages under nonequilibrium dynamic conditions and that the aforementioned polyyne chains play a crucial role in the self-organization process. (1) First occurs *nucleation* of polycyclic structures from entangled polyyne chains (irreversible carbon sp^2 re-hybridization from sp-hybridized polyynes, formed by the party line mechanism). (2) The nucleation step is followed by *growth* which utilizes the familiar ring condensation of carbon chains and rings attached to the hexagon and pentagon containing nucleus (similar to Rubin's proposed ring condensation mechanism[104] and Smalley's pentagon road[15]). (3) At the final stage, *cage closure* similar to the mechanisms observed for the self-capping mechanism of open-ended carbon nanotubes sets in,[165,167] where polyyne chains reach over the opening and "zip" them closed in analogy to the self-capping of open-ended single-walled nanotubes.

During the nucleation stage, long sp-hybridized carbon polyyne chains entangle and form initial clusters of condensed "small" rings (which we call nucleus) owing to random carbon fluctuations, which can attain lifetime long enough at around 2000 K to form bonds with neighboring carbon atoms of attached chains, thus creating larger condensed polyaromatic systems by the ring-collapse mechanism.[71,72] Nucleation can therefore be seen as amplification of random fluctuations as described by Prigogine for systems far from thermodynamic

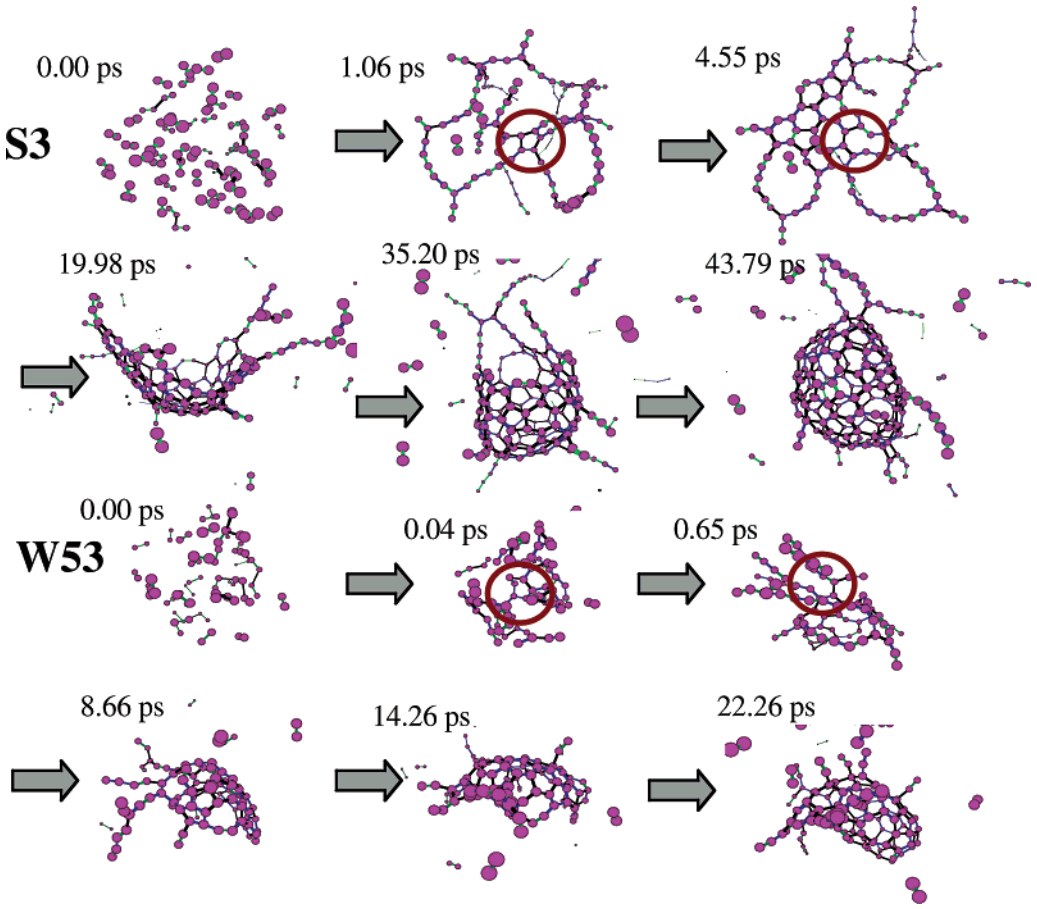

Figure 3. Snapshots of **S3** and **W53**, adapted from refs 153 and 155.

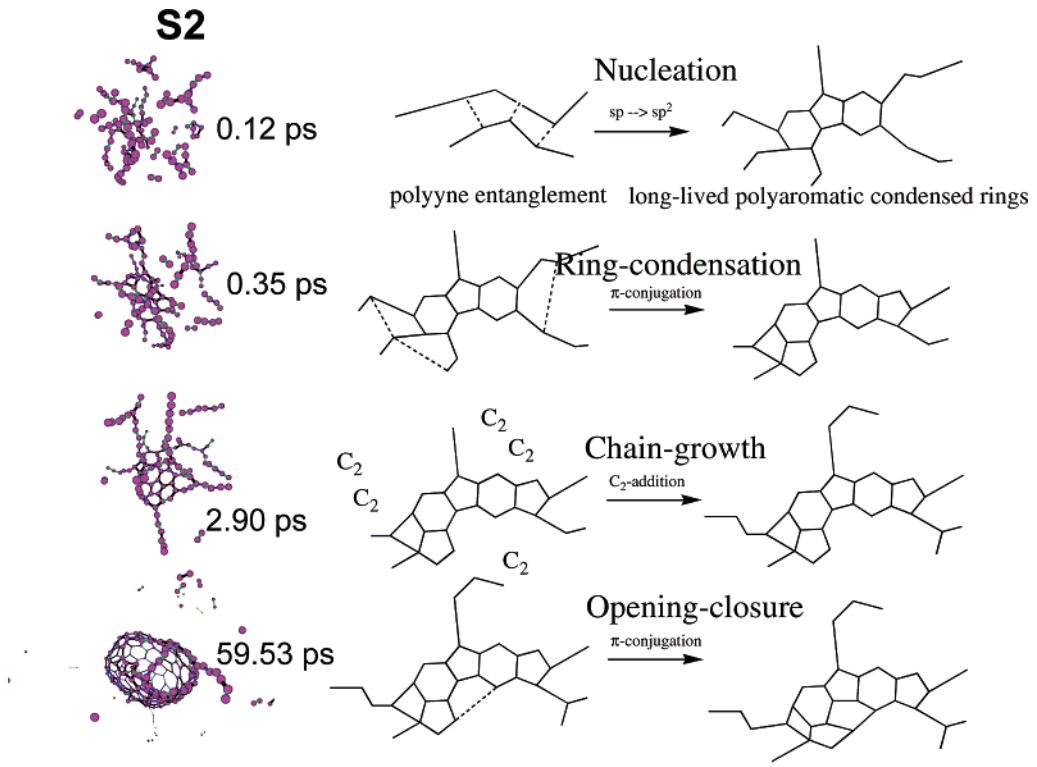

Figure 4. Trajectory snapshots from **S2** giant fullerene formation trajectory from ref 153 and schematic explanations of events during the simulation.

equilibrium. Due to its enormous exothermicity,[87] this sp to sp^2 re-hybridization step is irreversible, which means the only way structural conformations can be achieved from this point forward are ring size transformations similar to the 6/6/6/6 to 5/7/7/5 Stone−Wales mechanism.[27] During the entanglement process, we find that for geometric reasons four-membered rings are frequently formed, which however quickly isomerize to pentagons and hexagons. We found that the possibility for ring

destruction is greatly reduced once three or more hexagon or pentagon rings are forming a condensed ring system. At temperatures of 2000 K and higher, the energetic difference between pentagons and hexagons does not matter very much, and we found that both 5- and 6-membered rings are readily created with a ratio of about 1:1, respectively. Over time, this ratio approaches approximately 1:2 at 2000 K, favoring hexagons as a consequence of continued annealing.[153,155] While the growing condensed ring system lowers energy nonlinearly by growing π-delocalization, the embedded pentagons force the growing slab to adapt curvature. At the same time, attached polyyne chains are growing by catching additional C_n molecules from the carbon mixture of the environment and retain thereby their flexibility to bend so much that ring condensation between slab border atoms and the nearest chain neighbor atoms can continue to proceed. The interplay between growing polyyne chains through interaction with the environment and the irreversibly growing π-system and hence stability of the growing carbon slab is a prime example for an autocatalytic process, as discussed by Prigogine in the context of nonequilibrium thermodynamics and resulting self-organization processes.[105] The result of this pentagon-containing slab self-assembly is typically a basket-shaped carbon cluster with several long polyyne chains attached to its opening, and these chains are able to reach over to the other ends, forcing the system to eventually close to a fullerene cage. As a result, the self-assembled structure looks like a more or less spherical cage with remaining polyyne chains attached as "antennae" protruding out from the sphere, anchored by sp^3-hybridized carbon atoms embedded in the cage surface. This process is possible only if the system is properly thermostated, i.e., if the resulting heat from exothermic sp to sp^2 hybridization and the final cage closure is dissipated into the environment (thereby increasing the overall entropy while reducing the entropy of the cluster), which is almost certainly the reason experimentally no fullerenes are found if no carrier gas is present.[172]

The energy profile associated with this overall self-assembly mechanism is constantly downhill, because catching high-energetic small carbon fragment molecules and forming bonds to attach them at the attached carbon chains constantly releases energy. It is straightforward to see that the curvature of GFs is less steep than that of C_{60} or C_{70}, and that therefore large reaction barriers as observed in the self-folding of C_n clusters with small n do not occur,[112−114] and our prediction that at first the large cousins of BF and C_{70} are created makes perfect sense from this point of view, as well as in the light of the GF abundance during experimental fullerene formation.

To confirm the accuracy of our DFTB-based QM/MD simulations, we have followed the energetics of **S3**[153] low-density and **W53**[155] high-density trajectories stepwise in time intervals of 1 ps by single-point ab initio PBE/3-21G density functional calculations in a forthcoming study, and we have confirmed that the PES landscape with the energy of noninteracting C_2 molecules as reference during the self-assembly process looks identical at both DFTB and PBE levels of theory.

Interestingly, the size-up part of the "shrinking hot giant" road of fullerene formation points to a combination of "party line" at initial stages, where multiple C_2 units spontaneously join to form longer polyyne chains, and a variant of the "ring-collapse" mechanism called "ring-condensation", first formulated by Rubin et al.[104] but of course related to the ring fusion spiral zipper mechanism of van Helden, Hunter, and others,[71,72,95−97] with growing graphene bowls reminiscent of the pentagon road [15,28,91] as main actors.

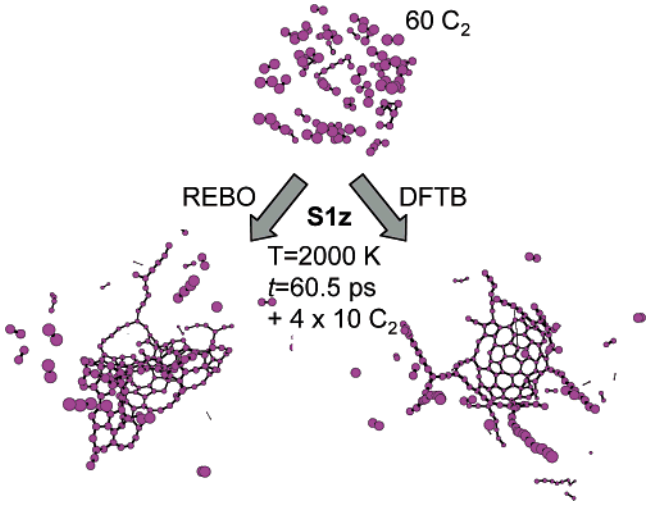

Figure 5. S1z trajectory of the same random ensemble of 60 C_2 molecules in a 30 Å^3 periodic boundary box after heating to 2000 K and 4 times addition of 10 C_2 units in 12.1 ps intervals. Total simulation time at this stage is 60.5 ps.

Role of Initial Carbon Density and Type of Carbon Fragments. As mentioned, one of the parameters varied in our size-up simulations was the carbon density. We find that high initial carbon densities seem to be helpful in causing a greater degree of three-dimensional (3D) entanglement between branched carbon chains. Such 3D scaffolds can act as sp-to-sp^2 re-hybridization seed, along which ring condensation growth of a more curved graphene sheet can take place. However, the much reduced fullerene cage yield (only 5% as opposed to 20% to 30% in the low-density cases) indicates that possibly other defects such as sp^3-hybridizations and out-of-control growth (sprawling) can frequently occur with high carbon densities. A corroborating experimental observation is the effectiveness of He as opposed to Ne or Ar as carrier gas, since He expands the carbon vapor plume faster than any other gas, and leads distinctively to higher fullerene yields.[89,172,173]

We have also tried different carbon fragments as feedstock molecules, for instance C_6 tridehydrobenzene hexagons; however, we have not seen accelerated growth due to this change. In fact, C_6 rings are unstable toward ring opening, and immediately polyyne chains are formed as initial reaction systems, similar to the case of C_2 molecules.

Importance of Quantum Chemical Potential for Fullerene Formation. We demonstrated that the use of REBO as potential in MD simulations can lead to qualitatively wrong intermediate structures that contain many sp^3 defects (see Figure 5), and the fact that purely local potentials do not consider the effect of delocalized π-electronic states leads to a poor description of graphite's amazing self-healing capabilities, and consequently to significantly overestimated formation time scales. This discrepancy is apparent when one compares the time scale of Maruyama's fullerene formation REBO MD simulations, which is on the order of nanoseconds,[140−143] with our QM/MD fullerene formation simulation, where giant fullerenes are grown within 40 to 100 ps, i.e., about 100−500 times faster for comparable target temperatures.

C. Shrinking of Hot Giant Fullerenes: Size-Down. In principle, larger fullerene cages are energetically preferable due to their lower steric strain energy, since aromaticity and thermodynamic stability considerations are not very important for the relative stabilities of different-size carbon clusters (see Introduction). However, the GFs are produced "hot", in a vibrationally highly excited state, due to the rapid gain of energy

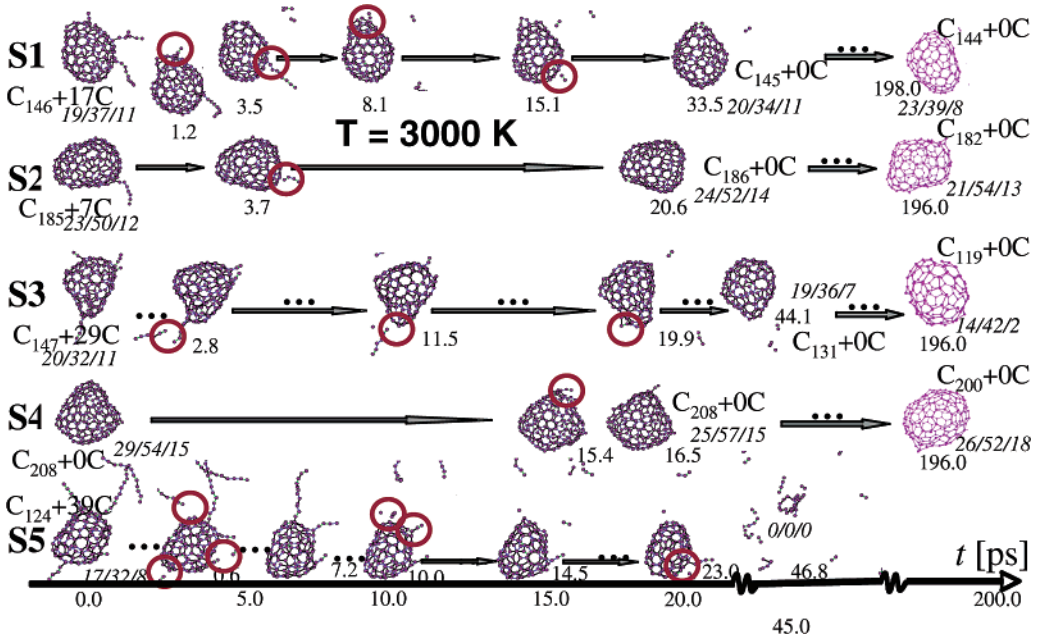

Figure 6. Summary of prolonged heating trajectories **S1** to **S5**. Roman number below each snapshot is the time *t* in ps; the time zero is the time the fullerene is formed. Special emphasis is placed on 0 to 20 ps. Some structures are slightly misplaced due to space restrictions. Red circles indicate locations of "falloff" or "pop-out" processes and are mentioned in the text. Numbers in italic next to starting and finishing snapshots are the numbers of pentagons/hexagons/heptagons, respectively. Labels $C_n + mC$ stands for fullerene cage of size *n* with *m* carbon atoms attached in side chains. Three black dots (...) between structures indicate additional events not shown in the figure. Partially from ref 155.

by cage closure, and this energy has to be dissipated, either by unimolecular decomposition or collision with other carbon clusters or carrier gas atoms. Our QM/MD simulations reveal that newly produced GFs inevitably shrink to smaller sizes, a process that is obviously related to the environmental temperature and the duration of heat exposure.

Prolonged Heating of Self-assembled Giant Fullerenes. In this section we present our results[155] of QM/MD simulations of vibrationally excited "hot" giant fullerenes that were created during the previously described "size-up" part of the shrinking hot giant road. The only difference in the computational methodology from our "size-up" simulations here is that we did not periodically add C_2 molecules and that periodic boundary conditions were dropped to allow expelled fragments to leave the surrounding area of the shrinking fullerenes.

Figure 6 illustrates the events encountered for prolonged heating of fullerene structures resulting from our five successful (**S1** to **S5**) trajectories,[153,155] starting with the corresponding C_{146}, C_{184}, C_{146}, C_{208}, and C_{124} fullerene cages for **S1** to **S5**, respectively. The simulation end (cage completion) times given in ref 153 are reset in Figure 1 to 0.00 ps for a more consistent discussion about events after cage closure. Results up to approximately 48 ps were reported in ref 155, with corresponding trajectories posted online at http://euch4m.chem.emory.edu/nano, and since then we have continued these size-down trajectories up to almost 200 ps. The temperature was chosen constant at 3000 K throughout these studies; 2000 K proved to be too uneventful in preliminary calculations, while for prolonged heating temperatures around 4000 and 5000 K fast cage disintegration was observed. During continued heating of these GFs at 3000 K we noticed two fundamentally different modes of cluster size reduction: "falloff" of side-chains attached to the fullerene cages, and "pop-out" of C_2 fragments from within the cage walls. The latter process is easily recognizable as "shrink-wrap" C_2 elimination; however, this cage-size reducing mechanism has never before been mentioned in the context of fullerene formation. Included in the term "falloff" are shortening processes of attached side-chains, which are also observed frequently. These two processes can be considered as key elements in annealing processes when hot fullerene molecules are gradually cooling. We performed similar prolonged heating trajectories for the 5 successfully formed **W** cages, and because the system size here is somewhat smaller, we have been able to perform simulations up to 400 ps and shrink the smallest cage **W40** from C_{74} down to C_{67}. It is very likely that bombardment of the hot GFs with fast noble gas atoms and collisions with other carbon clusters increases the number of both "falloff" as well as "pop-out" events and hence the overall shrinking rate, but we did not include multibody effects in our QM/MD simulations thus far.

Falloff Events. Driving force for the "antennae" falloff at the early stages of GF shrinking is a combination of π-conjugation energy gain when the antenna anchoring atom on the fullerene cage can re-hybridize from sp^3 to sp^2, but also simply the large amplitude motions of the antenna polyyne chains at the continued heating temperatures, which leads to a high overall probability for bond-breaking due to repeated violent wagging and stretch vibrations. We have generally observed that antennae fall off within 3 ps to 30 ps at 3000 K and 50 to 100 ps at 2000 K depending on their number and the bond breaking sequence (see Figure 7). In either case the GF sheds off the bulky polyyne chains rather quickly, in effect assuming a more stable spherical shape at these high temperatures. If antennae break somewhere along the sp-chain leaving very short antennae attached to the cage surface, their lifetime can be considerably longer.

Pop-out Events. A detailed description of "pop-out" events for prolonged heating trajectory **S3** was given in ref 155, and we arrived in this work at the conclusion that such events perhaps occur on the order of 1 C per picosecond. We noticed that prerequisite for the formation of a pop-out C_2 unit is violent motion concentrated in a specific part of giant fullerenes, and that these motions occasionally set "wobbling C_2" units free, leaving a radical center at the other end of the now opened cage. When pop-out happens, π-delocalization in that particular area is temporarily interrupted, and if the defect does not quickly heal, more σ-type bonds break in the vicinity of this defect, so

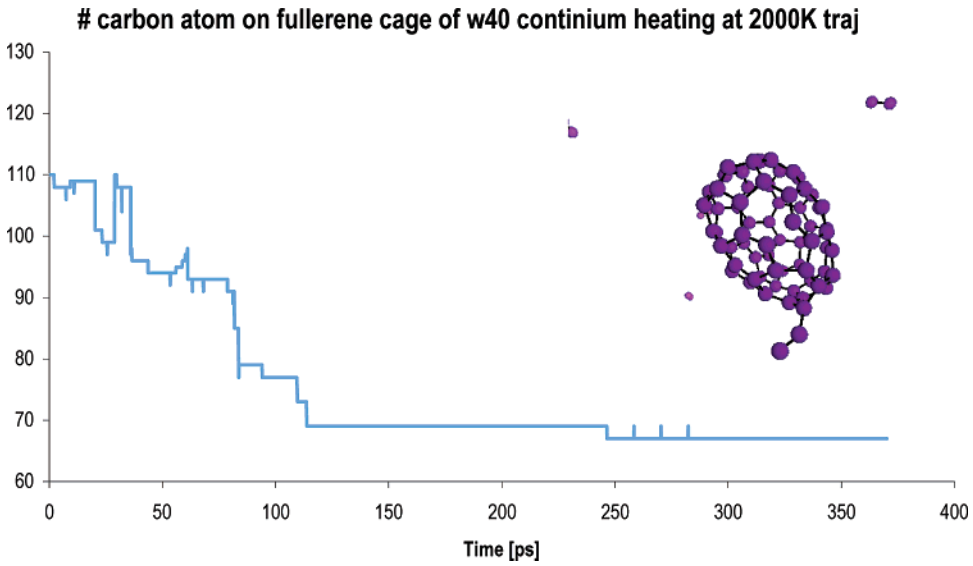

Figure 7. Prolonged heating of **W40** after self-assembly at 2000 K. Falloff is mainly occurring up until 80 ps, after which the original 74 carbon cage shrinks via the pop-out mechanism.

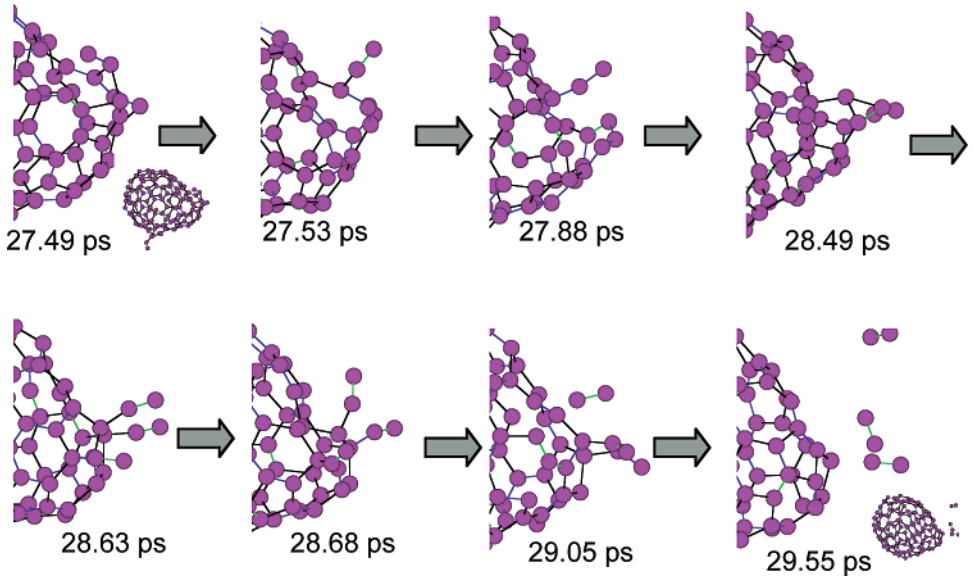

Figure 8. Snapshots of three almost simultaneous pop-out events at a kink of **S3**. Small insets show entire carbon cage.

that double-pop-out can occur as well. Figure 8 shows a such a pop-out snapshot sequence for the prolonged heating of **S3**.

Since then we noticed in additional prolonged heating trajectories that pop-out may in fact occur most prominently in the area of GF kinks, where the large amplitude cage vibrations are leading most prominently to significant C−C stretch vibrations, while in the more spherical parts of the molecule breathing modes prevail. Not surprisingly, these kinks are therefore associated with frequent Stone−Wales type isomerizations, not rarely leading to eight-membered rings to ease the strain energy due to the kink. These large-ring defects are then very prone to C_2 pop-out, leading to a smoothing of the kink in this area of the cage. As the GF shrinks and becomes more and more spherical, such pop-out events occur more and more rarely, and the shrinking is significantly slowed, perhaps on an exponential time scale. Since these trajectories are computationally very expensive, we have not enough data to reliably give estimates for the time dependence of the GF shrinking process, but it *does* occur naturally in our simulations and is obviously a thermal variation of the original laser-induced shrink-wrap mechanism.[15,28,29] Since the reverse reaction, C_2 insertion is a quasi-elastic process if the reaction heat cannot be absorbed by a third body,[127,128] the size-down part of the shrinking hot fullerene road is also a strictly irreversible process. Recently, endohedral metallfullerenes with carbide entrapped inside the cage have been increasingly reported,[174−176] and we ascribe the existence of these C_2 units inside the fullerene cage to a "suck-in" rather than "pop-out" process, due to the presence of the positively charged metal cations and the weakening of the cage's π network as a result of charge transfer. A further indirect experimental confirmation of the shrinking process can be seen in the fact that guest-clusters of different symmetry such as Sc_3N (three-fold rotational symmetry) and Sc_2C_2 (two-fold rotational symmetry) impose different symmetries on the most stable isomers of the host fullerenes if they are small enough, e.g., $Sc_3N@C_{68}$ (isomer 6140, D_3 symmetry)[177] and $Sc_2C_2@C_{68}$ (isomer 6073, C_{2v} symmetry).[178] Here, the shrinking process leads to "slinky" carbon cages wrapped tightly around the guest molecules.

Comparison with Experimental Fullerene Size Distributions. First we note that obviously the rate of GF shrinking and therefore the yield of C_{60} over GFs depends on temperature and

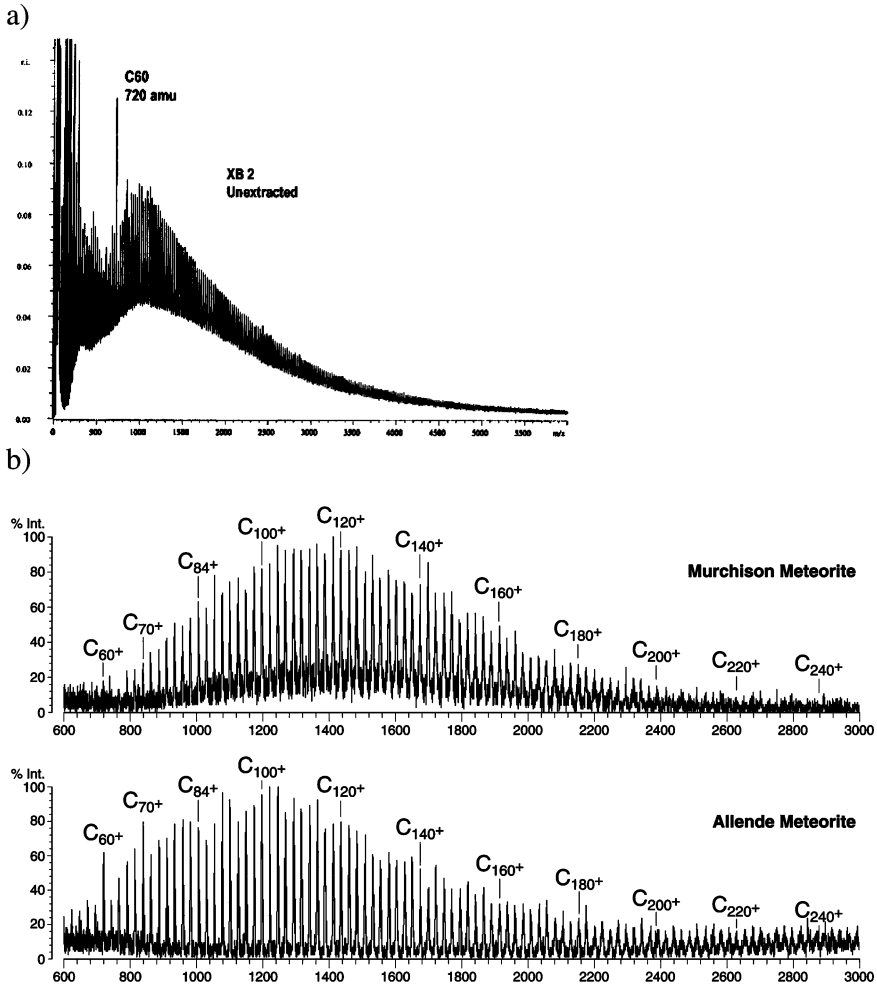

Figure 9. (a) Fullerene size-distribution in petroleum feedstock combustion method. Used with permission from ref 78. (b) Fullerenes C60, C70, and GFs in mass spectra of fullerenes found in the Murchinson and Allende Meteorites. Used with permission from ref 180.

the duration of heating. For GFs to assemble, it is necessary to allow polyyne chains to nucleate, which we found occurs most successfully at around 2000 K. On the other hand, 3000 K accelerates pop-out events, leading to faster shrinking. In experiment of course, the carrier gas kinetic energy follows uniformly a Boltzmann distribution, and temperature is equally distributed throughout the reaction process. If one introduces directionality in the motion of the cooling carbon vapor, such as in the fullerene combustion synthesis, the growing clusters traverse from regions of high temperature (close to the flame) to low temperature (far away from the flame). In this sense, a 3D burner which maintains high heat during the time-of-flight better than a 2D burner should produce a higher C_{60} yield, and according to Nano-C, Inc. it obviously does so,[179] matching another puzzle piece for the complete picture of the shrinking hot giant road of fullerene formation.

On the other hand, if heat exposure time is short or the carbon material is not very concentrated, both size-up and size-down steps take considerably longer. Figure 9 shows size-distributions of fullerenes (a) under optimized conditions,[78] (b) as found in the Murchison and Allende meteorites.[180] If one assumes that the fullerenes found in the meteorites are products of carbon-rich molecular species heated during entry into the earth atmosphere or at impact, it appears that somehow GFs by far outweigh the yield of C_{60}, which appears only as a lesser product. It is possible that the heat exposure in this case was not uniform and long enough for the fullerenes to successfully shrink, a phenomenon that is also observed in the case of GFs occurring as byproduct of CVD-based SWNT production.[57,58] More clearly, Milani et al. have recently shown that, if no annealing occurs at all, the maximum of the resulting carbon cluster size distribution is located around 900.[156]

D. The Shrinking Hot Giant Road of Fullerene Formation: Emergent C_{60} and C_{70} Molecular Structures in Non-equilibrium Thermodynamics of Carbon Vapor. In light of the simulation results and discussions given above, one could say that the beautiful molecular structure of the highly ordered and symmetrical C_{60} molecule simply happens to be a consequence of the fact that it is the smallest member in the Goldberg series (which follows the IPR by construction) of near-spherical, icosahedral carbon cages with closed surface, a closed-shell electron configuration, and large energetic stabilization.[50] As such, it ideally combines all characteristics necessary for a molecular carbon cluster consisting of sp^2-hybridized carbon atoms to survive prolonged exposure to high temperatures in an open environment: spherical shape, singlet electronic ground state, no dangling bonds, and an almost unstrained sp^2-carbon network (only hexagons and pentagons with vertex bond angles close to 120°). Its structure emerges via a series of irreversible pop-out processes during the shrinking of newly formed, vibrationally excited giant fullerenes, which apparently stops at C_{60} due to its extraordinary high barrier of C_2 elimination to C_{58}. Since there is no IPR fullerene smaller than C_{60}, smaller cages, if formed, most likely disintegrate and become "recycled" in the size-up process. The giant fullerenes themselves dynamically self-assemble in a three-stage autocatalytic process from

polyyne chains during irreversible exothermic $sp \rightarrow sp^2$ rehybridization, where occasional pentagons incorporated in growing graphene sheets lend modest curvature to the growing superstructure, ultimately producing closed spherical cages without open edges or dangling bonds. Continued cage shrinking also explains how the large ring strain can be overcome, which is a large problem for the construction of C_{60} from only sixty carbon atoms, or even worse from even smaller cages (fullerene road) or carbon polycycles. Between most pop-out events, the fullerene cage has time to undergo Stone−Wales and related transformations that eventually may lead to the energetically most stable isomer, as Osawa[181] and Maruyama[143] have impressively shown before in generalized Stone−Wales (GSW) reaction pathway and REBO MD simulations, respectively. The I_h symmetric structure is therefore the ultimate survivor of a continued bombardment of giant fullerenes by carrier gas and other carbon fragments, which is where we meet at the beginning of both theoretical and experimental exploration of BF C_{60}: the soccer ball as archetype of a nearly round sphere with a minimum number of vertices. The argument for the abundance of the almost spherical, thermodynamically favorable closed-shell C_{70} fullerene (the C_{70}:C_{60} ratio is typically 0.1 to 0.3[6]) follows similar lines, in particular considering the fact that C_{60} and C_{70} are the only and therefore smallest IPR satisfying C_n fullerenes with $n \leq 70$. This fact clearly supports the validity of the continued size-down part of the shrinking hot giant road and the survival of the C_{60} and C_{70} species "of some nozzle process which is removing the other clusters from the beam," as Smalley et al. already suggested in their original works.[89]

6. Conclusion and Outlook

In conclusion, we hope to have shown that the individual puzzle pieces for the entire picture of fullerene formation have been known all along (polyyne chains, party line and pentagon roads, ring condensation, giant fullerenes, and shrink-wrap mechanism), but that it took a priori QM/MD simulations of randomly oriented C_2 molecules under high temperature and constant flux to simulate the conditions of hot carbon vapor to finally see how they fit together. We believe that the shrinking hot giant road of fullerene formation is a novel example of molecular dynamic self-assembly as described by Prigogine[105,157,158] and Whitesides,[182] makes sense in the light of the plethora of collected experimental findings, and that it is universally valid in general terms for all fullerene species, at least in its two-step aspect (size-up followed by size-down), including and especially for the soccer ball molecule buckminsterfullerene C_{60}.

From here, several tasks need to be addressed before the book can completely be closed on a complete QM/MD simulation of C_{60} formation. First, obviously, we have to simulate the shrinking process down to C_{60} in silico, following the size-down path, and currently we have arrived at C_{65} as smallest cage formed this way. Second, annealing needs to be performed to identify consistently with our previous simulations that the I_h structure can be achieved from a disordered hot C_{60} cage, but perhaps annealing and shrinking need to be addressed together. Third, we are currently performing simulations of PAH radicals to explain the size-up pathway in the case of hydrocarbon combustion synthesis, and fourth, the role of the carrier gas and occasional ionization needs to be addressed in QM/MD simulations. However, at this stage we are already fully confident that the C_{60} formation puzzle clearly reveals the "shrinking hot giant" road as a completed picture, since it is so remarkably simple and beautiful in its power to explain all experimental findings.

Acknowledgment. Dedicated to the memory of Richard E. Smalley. S.I. gratefully acknowledges a short term visiting fellowship from JSPS to Nagoya University. This work was partially supported by a grant from the Mitsubishi Chemical Corporation, and computer resources were provided in part by the Air Force Office of Scientific Research through a DURIP grant (FA9550-04-1-0321) and access to MSRC as well as by the Cherry L. Emerson Center of Emory University. We also thank the Pacific Northwest National Laboratory's EMSL and the Oak Ridge National Laboratory's Center for Nanophase Materials Sciences for valuable computer time.

References and Notes

(1) Osawa, E. In *International Fullerenes Workshop 2001*; Osawa, E., Ed.; Kluwer: Dordrecht, 2001; p xiii-xiv.
(2) Dresselhaus, M. S.; Dresselhaus, G.; Avouris, P. *Carbon Nanotubes: Synthesis, Structure, Properties, and Applications*; Springer: New York, 2001.
(3) Kroto, H. W.; Heath, J. R.; O'Brien, S. C.; Curl, R. F.; Smalley, R. E. *Nature* **1985**, *318*, 162−163.
(4) Rohlfing, E. A.; Cox, D. M.; Kaldor, A. *J. Chem. Phys.* **1984**, *81*, 3322−3330.
(5) Kroto, H. W.; Allaf, A. W.; Balm, S. P. *Chem. Rev.* **1991**, *91*, 1213−1235.
(6) Saito, S.; Oshiyama, A. *Phys. Rev. B* **1991**, *44*, 11532−11535.
(7) Krätschmer, W.; Lamb, L. D.; Fostiropoulos, K.; Huffman, D. R. *Nature* **1990**, *347*, 354−358.
(8) Krätschmer, W.; Fostiropoulos, K.; Huffman, D. R. *Chem. Phys. Lett.* **1990**, *170*, 167−170.
(9) Taylor, R.; Hare, J. P.; Abdul-Sada, A. K.; Kroto, H. W. *J. Chem. Soc. Chem. Commun.* **1990**, *1990*, 1423−1425.
(10) Shinohara, H.; Sato, H.; Saito, Y.; Takayama, M.; Izuoka, A.; Sugawara, T. *J. Phys. Chem.* **1991**, *95*, 8449−8451.
(11) So, H. Y.; Wilkins, C. *J. Phys. Chem.* **1989**, *93*, 1184−1187.
(12) Kroto, H. W.; McKay, K. *Nature* **1988**, *331*, 328−331.
(13) Kroto, H. W. *Pure Appl. Chem.* **1990**, *62*, 407−415.
(14) Ugarte, D. *Nature* **1992**, *359*, 707−709.
(15) Smalley, R. E. *Acc. Chem. Res.* **1992**, *25*, 98−105.
(16) McKay, K. G.; Kroto, H. W.; Wales, D. J. *J. Chem. Soc., Faraday Trans.* **1992**, *88*, 2815−2821.
(17) Ajayan, P. M.; Ichihashi, T.; Iijima, S. *Chem. Phys. Lett.* **1993**, *202*, 384−388.
(18) Banhart, F. *J. Appl. Phys.* **1997**, *81*, 3440−3445.
(19) Hebgen, P.; Goel, A.; Howard, J. B.; Rainey, L. C.; van der Sande, J. B. *Proc. Comb. Institute* **2000**, *28*, 1397−1404.
(20) Ozawa, M.; Goto, H.; Kusunoki, M.; Osawa, E. *J. Phys. Chem. B* **2002**, *106*, 7135−7138.
(21) Fan, J.; Yudasaka, M.; Kasuya, D.; Azami, T.; Yuge, R.; Imai, H.; Kubo, Y.; Iijima, S. *J. Phys. Chem. B* **2005**, *109*, 10756−10759.
(22) Jin, Y. Z.; Gao, C.; Hsu, W. K.; Zhu, Y.; Huczko, A.; Bystrzejewski, M.; Roe, M.; Lee, C. Y.; Acquah, S.; Kroto, H. W.; Walton, D. R. M. *Carbon* **2005**, *43*, 1944−1953.
(23) O'Brien, S. C.; Heath, J. R.; Curl, R. F.; Smalley, R. E. *J. Chem. Phys.* **1988**, *88*, 220−230.
(24) Weiss, F. D.; Elkind, J. L.; O'Brien, S. C.; Curl, R. F.; Smalley, R. E. *J. Am. Chem. Soc.* **1988**, *110*, 4464−4465.
(25) O'Brien, S. C. Ph.D. Dissertation, Rice University, 1988.
(26) Stanton, R. E. *J. Phys. Chem.* **1992**, *96*, 111−118.
(27) Stone, A. J.; Wales, D. J. *Chem. Phys. Lett.* **1986**, *128*, 501−503.
(28) Curl, R. F.; Smalley, R. E. *Sci. Am.* **1991**, *265*, 54−63.
(29) Smalley, R. E. *Large Carbon Clusters*; American Chemical Society: Washington, DC, 1992; Vol. 481.
(30) Schwarz, H.; Weiske, T.; Böhme, D. K.; Hrusak, J. In *Buckminsterfullerenes*; Billups, W. E., Ciufolini, M. A., Eds.; VCH Publishers: New York, 1993.
(31) Callahan, J. H.; Ross, M. M.; Welske, T.; Schwarz, H. *J. Phys. Chem.* **1993**, *97*, 20−22.
(32) Ehlich, R.; Knospe, O.; Schmidt, R. *J. Phys. B: At. Mol. Opt. Phys.* **1997**, *30*, 5429−5449.
(33) Reinkoster, A.; Werner, U.; Lutz, H. O. *Europhys. Lett.* **1998**, *43*, 653−658.
(34) Chase, M. W., Jr. *NIST-JANAF Thermochemical Tables*, 4th ed.; NIST: Gaithersburg, MD, 1998.
(35) Lifshitz, C. *Int. J. Mass. Spectrom.* **2000**, *198*, 1−14.
(36) Osawa, E. *Kagaku* **1970**, *25*, 854−863.
(37) Yoshida, Z.; Osawa, E. *Aromaticity* Kyoto, 1971.
(38) Osawa, E. *Proc. Trans. Phys. Sci. Eng.* **1993**, *343*, 1−8.
(39) Bochvar, D. A.; Gal'pern, E. G. *Proc. Acad. Sci. USSR* **1973**, *209*, 239−241.

(40) Stankevich, I. V.; Nikerov, M. V.; Bochvar, D. A. *Russ. Chem. Rev.* **1984**, *53*, 640−655.
(41) Kroto, H. W. *Nature* **1987**, *329*, 529−531.
(42) Fowler, P. W.; Batten, R. C.; Manopoulous, D. E. *J. Chem. Soc., Faraday Trans.* **1991**, *87*, 3103−3104.
(43) Fowler, P. W.; Manopoulous, D. E.; Ryan, R. P. *Carbon* **1992**, *30*, 1235−1250.
(44) Aihara, J.; Hosoya, H. *Bull. Chem. Soc. Jpn.* **1988**, *61*, 2657−2659.
(45) Atkins, P. W. *Physical Chemistry* New York, 1990; Vol. Chapter 12.
(46) Rioux, F. *J. Chem. Educ.* **1994**, *71*, 464.
(47) Hirsch, A.; Chen, Z.; Jiao, H. *Angew. Chem., Int. Ed.* **2000**, *39*.
(48) Schleyer, P. v. R.; Maerker, C.; Dransfeld, A.; Jiao, H.; van Eikema Hommes, N. J. R. *J. Am. Chem. Soc.* **1996**, *118*, 6317−6318.
(49) Fowler, P. W.; Woolrich, J. *Chem. Phys. Lett.* **1986**, *127*, 78−83.
(50) Fowler, P. W. *Chem. Phys. Lett.* **1986**, *131*, 444−450.
(51) Newton, M. D.; Stanton, R. E. *J. Am. Chem. Soc.* **1986**, *106*, 2469−2470.
(52) Dunlap, B. I.; Boettger, J. C. *J. Phys. B: At. Mol. Opt. Phys.* **1996**, *29*, 4907−4913.
(53) Dunlap, B. I. *Int. J. Quantum Chem.* **1997**, *64*, 193−203.
(54) Cataldo, F.; Keheyan, Y. *Fullerenes, Nanotubes, Carbon Nanostruct.* **2002**, *10*, 313−332.
(55) Gerhardt, P.; Löffler, S.; Homann, K.-H. *Chem. Phys. Lett.* **1987**, *137*, 306−310.
(56) Howard, J. B.; McKinnon, J. T.; Makarovsky, Y.; Lafleur, A. L.; Johnson, M. E. *Nature* **1991**, *352*, 139−141.
(57) Ramesh, S.; Brinson, B.; Johnson, M. P.; Gu, Z.; Saini, R. K.; Willis, P.; Marriott, T.; Billups, W. E.; Margrave, J. L.; Hauge, R. H.; Smalley, R. E. *J. Phys. Chem. B* **2003**, *107*, 1360.
(58) Sadana, A. K.; Liang, F.; Brinson, B.; Arepalli, S.; Farhat, S.; Hauge, R. H.; Smalley, R. E.; Billups, W. E. *J. Phys. Chem. B* **2005**, *109*, 4416.
(59) Becker, L.; Bada, J. L.; Winans, R. E.; Hunt, J. E.; Bunch, T. E.; French, B. M. *Science* **1994**, *265*, 642−645.
(60) Becker, L.; Bada, J. L.; Winans, R. E.; Bunch, T. E. *Nature* **1994**, *372*, 507.
(61) Becker, L.; Poreda, R. J.; Hunt, A. G.; Bunch, T. E.; Rampino, M. *Science* **2001**, *291*, 1530−1533.
(62) Daly, T. K.; Buseck, P. R.; Williams, P.; Lewis, C. F. *Science* **1993**, *259*, 599−601.
(63) Buseck, P. R.; Tsipursky, S. J.; Hettich, R. *Science* **1992**, *257*, 215−217.
(64) Heymann, D.; Chibante, L. P. F.; Brooks, R. R.; Wolbach, W. S.; Smalley, R. E. *Science* **1994**, *265*, 645−647.
(65) Gerhardt, P.; Loffler, S.; Homann, K. H. *Chem. Phys. Lett.* **1987**, *137*, 306−310.
(66) Heath, J. R.; Zhang, Q.; O'Brien, S. C.; Curl, R. F.; Kroto, H. W.; Smalley, R. E. *J. Am. Chem. Soc.* **1987**, *109*, 359−363.
(67) Kroto, H. W.; Heath, J. R.; O'Brien, S. C.; Curl, R. F.; Smalley, R. E. *Astrophys. J.* **1987**, *314*, 352−355.
(68) Martin, J. M. L.; Francois, J. P.; Gijbels, R. *J. Chem. Phys.* **1991**, *95*, 9420−9421.
(69) Martin, M. *J. Photochem. Photobiol. A, Chem.* **1992**, *60*, 263−289.
(70) Ebbesen, T. W.; Tabuchi, J.; Tanigaki, K. *Chem. Phys. Lett.* **1992**, *191*, 336−338.
(71) van Helden, G.; Gotts, N. G.; Bowers, M. T. *Nature* **1993**, *363*, 60−63.
(72) Hunter, J.; Fye, J.; Jarrold, M. F. *Science* **1993**, *260*, 784−786.
(73) Song, X.; Bao, Y.; Urdahl, R. S.; Gosine, J. N.; Jackson, W. M. *Chem. Phys. Lett.* **1994**, *217*, 216−221.
(74) Gingerich, K. A.; Finkbeiner, H. C.; Schmude, R. W., Jr. *J. Am. Chem. Soc.* **1994**, *116*, 3884−3888.
(75) Krajnovich, D. J. *J. Chem. Phys.* **1995**, *102*, 726−743.
(76) Kruse, T.; Roth, P. *J. Phys. Chem. A* **1997**, *101*, 2138−2146.
(77) Arepalli, S.; Nikolaev, P.; Holmes, W.; Scott, C. D. *Appl. Phys. A* **2000**, *70*, 125−133.
(78) Johnson, M. P.; Donnet, J. B.; Wang, T. K.; Wang, C. C.; Locke, R. W.; Brinson, B. E.; Marriott, T. *Carbon* **2002**, *40*, 189−194.
(79) Burakov, V. S.; Bokhonov, A. F.; Nedel'ko, M. I.; Savastenko, N. A.; Tarasenko, N. V. *J. Appl. Spectrosc.* **2002**, *69*, 907−912.
(80) Sasaki, K.; Wakasaki, T.; Matsui, S.; Kadota, K. *J. Appl. Phys.* **2002**, *91*, 4033−4039.
(81) Nicolas, C.; Shu, J.; Peterka, D. S.; Hochlaf, M.; Poisson, L.; Leone, S. R.; Ahmed, M. *J. Am. Chem. Soc.* **2005**, *128*, 220−226.
(82) Nemes, L.; Keszler, A. M.; Parigger, C. G.; Hornkohl, J. O.; Michelsen, H. A.; Stakhursky, V. *Internet Electron. J. Mol. Des.* **2006**, *5*, 150−167.
(83) Kroto, H. W. *Carbon* **1992**, *30*, 1139−1141.
(84) Hutter, J.; Luthi, H. P.; Diederich, F. *J. Am. Chem. Soc.* **1994**, *116*, 750−756.
(85) van Orden, A.; Saykally, R. *Chem. Rev.* **1998**, *98*, 2313−2356.
(86) Zerbetto, F. *J. Am. Chem. Soc.* **1999**, *121*, 10958−10961.
(87) Wakabayashi, T.; Ong, A.-L.; Strelnikov, D.; Krätschmer, W. *J. Phys. Chem. B* **2004**, *108*, 3686−3690.
(88) Yamaguchi, Y.; Wakayashi, T. *Chem. Phys. Lett.* **2004**, *388*, 436−440.
(89) Zhang, Q. L.; O'Brien, S. C.; Heath, J. R.; Liu, Y.; Kroto, H. W.; Smalley, R. E. *J. Phys. Chem.* **1986**, *90*, 525−528.
(90) Kroto, H. W. *Science* **1988**, *242*, 1139−1145.
(91) Haufler, R. E.; Chai, Y.; Chibante, L. P. F.; Conceicao, J.; Jin, C.; Wang, L.-S.; Maruyama, S.; Smalley, R. E. *Mater. Res. Soc. Symp. Proc.* **1991**, *206*, 627−637.
(92) Heath, J. R. In *ACS Symposium Series*; Hammond, G. S., Kuck, V. J., Eds.; American Chemical Society: Washington, DC, 1991; Vol. 481, pp1−23.
(93) Wakabayashi, T.; Achiba, Y. *Chem. Phys. Lett.* **1992**, *190*, 465−468.
(94) Wakabayashi, T.; Shiromaru, H.; Kikuchi, K.; Achiba, Y. *Chem. Phys. Lett.* **1993**, *201*, 470−474.
(95) Schwarz, H. *Angew. Chem., Int. Ed. Engl.* **1993**, *32*, 1412−1415.
(96) Hunter, J. M.; Fye, J. L.; Roskamp, E. J.; Jarrold, M. F. *J. Phys. Chem.* **1994**, *98*, 1810−1818.
(97) Lagow, R. J.; et al.*Science* **1995**, *267*, 362−367.
(98) Ashkabov, A. M. *Phys. Solid State* **2004**, *47*, 1186−1190.
(99) Dravid, V. P.; Lin, X.; Wang, Y.; Wang, X. K.; Yee, A.; Ketterson, J. B.; Chang, R. P. H. *Science* **1993**, *259*, 1601−1604.
(100) Goroff, N. S. *Acc. Chem. Res.* **1996**, *29*, 77−83.
(101) Lozovik, Y. E.; Popov, A. M. *Physics − Uspekhi* **1997**, *40*, 717−737.
(102) Yamaguchi, Y.; Maruyama, S. In *11th International Heat Transfer Conference*, Kyongju, Korea, 1998; Vol. 4, pp 301−306.
(103) Bunz, U. H. F.; Rubin, Y.; Tobe, Y. *Chem. Soc. Rev.* **1999**, *28*, 107−119.
(104) Rubin, Y.; Diederich, F. In *Stimulating Concepts in Chemistry*; Vögtle, F., Stoddart, J. F., Masakatsu, S., Eds.; Wiley-VCH: Weinheim, 2000, pp 163−186.
(105) Prigogine, I.; Stengers, I. *Order out of Chaos: Man's new dialogue with nature*; Bantam Books: Toronto, 1984.
(106) Homann, K. H. *Angew. Chem., Int. Ed. Engl.* **1998**, *37*, 2435−2451.
(107) Baum, T.; Loffler, S.; Loffler, P.; Weilmunster, P.; Homann, K. H. *Ber. Bunsen-Ges. Phys. Chem.* **1992**, *96*, 841−857.
(108) Hausmann, M.; Hebgen, P.; Homann, K. H. *Symp. Int. Combust. Proc.* **1992**, *24*, 793−801.
(109) Gerhardt, P.; Löffler, S.; Homann, K.-H. *Proc. Combust. Inst.* **1989**, *22*, 395−401.
(110) van Helden, G.; Hsu, M.-T.; Gotts, N.; Boweres, M. T. *J. Phys. Chem.* **1993**, *97*, 8182−8192.
(111) Dewar, M. J. S.; Zoebisch, E. G.; Healy, E. F.; Stewart, J. J. P. *J. Am. Chem. Soc.* **1985**, *107*, 3902−3909.
(112) Mishra, R. K.; Lin, Y.-T.; Lee, S.-L. *J. Chem. Phys.* **2000**, *112*, 6355−6364.
(113) Lin, W.-H.; Tu, C.-C.; Lee, S.-L. *Int. J. Quantum Chem.* **2005**, *103*, 355−368.
(114) Lin, W.-H.; Lee, S.-L. *Chem. Phys. Lett.* **2004**, *393*, 222−227.
(115) Strout, D. L.; Scuseria, G. E. *J. Phys. Chem.* **1996**, *100*, 6492−6498.
(116) Bates, K. R.; Scuseria, G. E. *J. Phys. Chem. A* **1997**, *101*, 3038−3042.
(117) Jones, R. O. *J. Chem. Phys.* **1999**, *110*, 5189−5200.
(118) Portmann, S.; Galbraith, J. M.; Schaefer, H. F.; Scuseria, G. E.; Lüthi, H. P. *Chem. Phys. Lett.* **1999**, *301*, 98−104.
(119) Girifalco, L. A.; Lad, R. A. *J. Chem. Phys.* **1956**, *25*, 693.
(120) Diogo, H. P.; Minas da Piedade, M. E.; Dennis, T. J. S.; Hare, J. P.; Kroto, H. W.; Taylor, R.; Walton, D. R. M. *J. Chem. Soc., Faraday Trans.* **1993**, *89*, 3541−3544.
(121) Takano, K.; Mihashi, M.; Hirano, T. *Fullerene Sci. Technol.* **1998**, *6*, 283−299.
(122) An, W.; Gao, Y.; Sulusu, S.; Zeng, X. C. *J. Chem. Phys.* **2005**, *122*, 204109/1−204109/8.
(123) Sokolova, S.; Lüchow, A.; Anderson, J. B. *Chem. Phys. Lett.* **2000**, *323*, 229−233.
(124) Grimme, S.; Mück-Lichtenfeld, C. *Chem. Phys. Chem.* **2002**, *3*, 207−209.
(125) Boese, A. D.; Scuseria, G. E. *Chem. Phys. Lett.* **1998**, *294*, 233−236.
(126) Hennrich, F. H.; Eisler, H. J.; Gilb, S.; Gerhardt, P.; Wellmann, R.; Schulz, R.; Kappes, M. M. *Ber. Bunsen-Ges. Phys. Chem.* **1997**, *101*, 1605−1612.
(127) Budyka, M. F.; Zyubina, T. S.; Rabenko, A. G.; Muradyan, V. E.; Esipov, S. E.; Cherepanova, N. I. *Chem. Phys. Lett.* **2002**, *354*, 93−99.

(128) Budyka, M. F.; Zyubina, T. S.; Ryabenko, A. G. *Int. J. Quantum Chem.* **2002**, *88*, 652−662.
(129) van Duin, A. C. T.; Dasgupta, S.; Lorant, F.; Goddard, W. A., III *J. Phys. Chem. A* **2001**, *105*, 9396−9409.
(130) Brenner, D. W. *Phys. Rev. B* **1990**, *42*, 9458−9471.
(131) Brenner, D. W.; Harrison, J. A.; White, C. T.; Colton, R. J. *Thin Solid Films* **1991**, *206*, 220−223.
(132) Brenner, D. W. *Phys. Rev. B* **1992**, *46*, 1948.
(133) Brenner, D. W. *Phys. Status Solidi B* **2000**, *217*, 23−40.
(134) Stuart, S. J.; Tutein, A. B.; Harrison, J. A. *J. Chem. Phys.* **2000**, *112*, 6472−6486.
(135) Brenner, D. W.; Shenderova, O. A.; Harrison, J. A.; Stuart, S. J.; Ni, B.; Sinnott, S. B. *J. Phys. Cond. Matter* **2002**, *14*, 783−802.
(136) Ballone, P.; Milani, P. *Phys. Rev. B* **1990**, *42*.
(137) Robertson, D. H.; Brenner, D. W.; White, C. T. *J. Phys. Chem.* **1992**, *96*, 6133−6135.
(138) Chelikowsky, J. R. *Phys. Rev. B* **1992**, *45*, 12062−12070.
(139) Schweigert, V. A.; Alexandrov, A. L.; Morokov, Y. N.; Bedanov, V. M. *Chem. Phys. Lett.* **1995**, *235*, 221−229.
(140) Yamaguchi, Y.; Maruyama, S. *Trans. JSME* **1997**, *63−611B*, 2298−2404.
(141) Maruyama, S.; Yamaguchi, Y. *Trans. JSME* **1997**, *63−611B*, 2405−2412.
(142) Yamaguchi, Y.; Maruyama, S. *Chem. Phys. Lett.* **1998**, *286*, 336−342.
(143) Maruyama, S.; Yamaguchi, Y. *Chem. Phys. Lett.* **1998**, *286*, 343−349.
(144) Hua, X.; Cagin, T.; Che, J.; Goddard, W. A., III *Nanotechnology* **2000**, *11*, 85−88.
(145) Izekov, S.; Violi, A.; Voth, G. A. *J. Phys. Chem. B* **2005**, *109*, 17019−17024.
(146) Violi, A.; Truong, T. N.; Sarofim, A. F. *J. Phys. Chem. A* **2004**, *108*, 4846−4852.
(147) Fukui, K.; Yonezawa, T.; Haruo, S. *J. Chem. Phys.* **1952**, *20*.
(148) Fukui, K. In *Nobel Lectures, Chemistry 1981−1990*; Frangsmyr, T., Malmstrom, B. G., Eds.; World Scientific Publishing: Singapore, 1992; pp 9−26.
(149) Wang, C. Z.; Xu, C. H.; Chan, C. T.; Ho, K. M. *J. Phys. Chem.* **1992**, *96*, 3563−3565.
(150) Laszlo, I. *Europhys. Lett.* **1998**, *44*, 741−746.
(151) Kroto, H. W. *Angew. Chem., Int. Ed. Engl.* **1992**, *31*, 111−129.
(152) Lee, I.-H.; Kim, H. *J. Chem. Phys.* **2004**, *120*, 4672−4676.
(153) Irle, S.; Zheng, G.; Elstner, M.; Morokuma, K. *Nano Lett.* **2003**, *3*, 1657−1664.
(154) Irle, S.; Zheng, G.; Elstner, M.; Morokuma, K. In *Theory and Applications of Computational Chemistry: The First 40 Years*; Dykstra, C. E., Ed.; Seoul, Korea, 2004.
(155) Zheng, G.; Irle, S.; Morokuma, K. *J. Chem. Phys.* **2005**, *122*, 014708.
(156) Bogana, M.; Ravagnan, L.; Casari, C. S.; Zivelonghi, A.; Baserga, A.; Bassi, A. L.; Bottani, C. E.; Vinati, S.; Salis, E.; Piseri, P.; Barborini, E.; Colombo, L.; Milani, P. *New J. Phys.* **2005**, *7*, 1−8.
(157) Nicolis, G.; Prigogine, I. *Self-Organization in Nonequilibrium Systems: From Dissipative Structures to Order Through Fluctuations*; Wiley: New York, 1977.
(158) Prigogine, I. *The End of Certainty − Time, Chaos, and the New Laws of Nature*; The Free Press: New York, 1997.
(159) Field, R. J.; Koros, E.; Noyes, R. M. *J. Am. Chem. Soc.* **1972**, *94*, 8649−8664.
(160) Ahlers, G.; Cannell, D. S.; Steinberg, V. *Phys. Rev. Lett.* **1985**, *54*, 1373−1376.
(161) Porezag, D.; Frauenheim, T.; Köhler, T.; Seifert, G.; Kaschner, R. *Phys. Rev. B* **1995**, *51*, 12947−12957.
(162) Seifert, G.; Porezag, D.; Frauenheim, T. *Int. J. Quantum Chem.* **1996**, *58*, 185−192.
(163) Elstner, M.; Porezag, D.; Jungnickel, G.; Elsner, J.; Haugk, M.; Frauenheim, T.; Suhai, S.; Seifert, G. *Phys. Rev. B* **1998**, *58*, 7260−7268.
(164) Kohler, C.; Seifert, G.; Gerstmann, U.; Elstner, M.; Overhof, H.; Frauenheim, T. *Phys. Chem. Chem. Phys.* **2001**, *3*, 5109−5114.
(165) Zheng, G.; Irle, S.; Elstner, M.; Morokuma, K. *J. Phys. Chem. A* **2004**, *108*, 3182−3194.
(166) Zheng, G.; Irle, S.; Morokuma, K. *Chem. Phys. Lett.* **2005**, *412*, 210−216.
(167) Irle, S.; Zheng, G.; Elstner, M.; Morokuma, K. *Nano Lett.* **2003**, *3*, 465−470.
(168) Charlier, J.-C.; De Vita, A.; Blase, X.; Car, R. *Science* **1997**, *275*, 646−649.
(169) Zhao, X.; Ando, Y.; Liu, Y.; Jinno, M.; Suzuki, T. *Phys. Rev. Lett.* **2003**, *90*, 187401/1−187401/4.
(170) Fantini, C.; Cruz, E.; Jorio, A.; Terrones, M.; Terrones, H.; Van Lier, G.; Charlier, J.-C.; Dresselhaus, M. S.; Saito, R.; Kim, Y. A.; Hayashi, T.; Muramutsu, H.; Endo, M.; Pimenta, M. A. *Phys. Rev. Lett.* **2006**, submitted.
(171) Wang, Z.; Irle, S.; Morokuma, K.; University of Tokyo: Tokyo, 2005.
(172) Guangshi, T.; Hengjian, Z.; Chuanbao, C.; Rongzhi, L.; Hesun, Z. *J. Beijing Inst. Technol.* **1995**, *4*, 141−147.
(173) He, Y.; Xinmin, X.; Zhang, H.; Liang, Y. *Guangdong Gongye Daxue Xuebao* **1997**, *14*, 32−35.
(174) Wang, C.-R.; Kai, T.; Tomyama, T.; Yoshida, T.; Kobayashi, Y.; Nishibori, E.; Takata, M.; Sakata, M.; Shinohara, H. *Angew. Chem., Int. Ed.* **2001**, *113*, 411−413.
(175) Inoue, T.; Tomiyama, T.; Sugai, T.; Shinohara, H. *Chem. Phys. Lett.* **2003**, *382*, 226−231.
(176) Iiduka, Y.; Wakahara, T.; Nakahodo, T.; Tsuchiya, T.; Sakuraba, A.; Maeda, Y.; Akasaka, T.; Yoza, K.; Horn, E.; Kato, T.; Liu, M. T. H.; Mizorogi, N.; Kobayashi, K.; Nagase, S. *J. Am. Chem. Soc.* **2005**, *127*, 12500−12501.
(177) Stevenson, S.; Fowler, P. W.; Heine, T.; Duchamp, J. C.; Rice, G.; Glass, T.; Harich, K.; Hajdull, E.; Bible, R.; Dorn, H. C. *Nature* **2000**, *408*, 427−428.
(178) Shi, Z.-Q.; Wu, X.; Wang, C.-R.; Lu, X.; Shinohara, H. *Angew. Chem., Int. Ed.* **2006**, *45*, 2107−2111.
(179) Nano-C *Masters of the Flame: Industrial Production of Fullerenes Becomes a Reality*; http://www.nano-c.com/technologies.asp, 2004.
(180) Becker, L. In *31st Lunar and Planetary Science Conference*; Lunary and Planetary Institute: Houston, TX, 2000; Vol. 1000, p 1803.
(181) Osawa, E.; Ueno, H.; Yoshida, M.; Slanina, Z.; Zhao, X.; Nishiyama, M.; Saito, H. *J. Chem. Soc., Perkin Trans. 2* **1998**, *1998*, 943−950.
(182) Whitesides, G. M.; Grzybowski, B. *Science* **2002**, *295*, 2418−2421.